FORSCHUNGSZENTRUM
ROSSENDORF e.V.

FZR

FZR-76
March 1995

Gy. Ézsöl, A. Guba, L. Perneczky,
H.M. Prasser, F. Schäfer and E. Krepper

1% Cold leg break experiment on PMK-2 Test results and computer code analysis

Forschungszentrum Rossendorf e.V.
Postfach 51 01 19 · D-01314 Dresden
Bundesrepublik Deutschland

Telefon (0351) 591 2069
Telefax (0351) 591 2383
E-Mail schaeffr@fz-rossendorf.de

Gy. Ézsöl [1)]
A. Guba [1)]
L. Perneczky [1)]
H.-M. Prasser [2)]
F. Schäfer [2)]
E. Krepper [2)]

1) KFKI - Atomic Energy Research Institute, Hungary
2) FZR - Research Center Rossendorf, Germany

1% Cold leg break experiment on PMK-2 Test results and computer code analysis

Contents

1.	Introduction	3
2.	Facility description	3
3.	Experiment description	11
3.1	Measured initial conditions	11
3.2	Sequence of events	12
4.	Results and discussion	13
5.	ATHLET calculations	27
5.1	Modelling of the experiment	27
5.2	Results	28
6.	RELAP5 calculations	35
6.1	Modelling of the experiment	35
6.2	Results	38
7.	Comparison of the results	40
8.	Conclusions	41
9.	References	42

1. Introduction

In the framework of the computer code assessment programme for the VVER-440 type Paks Nuclear Power Plant a 1% cold leg break experiment has been conducted on the PMK-2 integral type test facility [1]-[4]. It was followed by calculations using RELAP 5Mod3.1 and ATHLET in order to assess code capabilities.

This experiment was started from the nominal operational parameters and it was considered that only the high pressure injection system (HPIS) is available and there is no injection from the safety injection tanks (SIT). This experiment was the repetition of the test measured in 1990 [5], with improved data aquisition system.

The first part of this report includes a short description of the facility, the measurement description, the test results including the local void measurement and a short interpretation of the main phenomena.

In the second part of the report the analysis performed by the RELAP 5Mod3.1 and ATHLET Mod1.1 Cycle A codes are given.

2. Facility description

A detailed description of the facility is given in [3] and [4]. The main features of the loop are described solely to contribute a better understanding of the test results. The volume and power scaling of the PMK-2 facility is 1:2070. Transients can be started from nominal operating conditions. The ratio of elevations is 1:1 except for the lower plenum and pressurizer. The six loops of the plant are modelled by a single active loop. On the secondary side of the steam generator, the steam/water volume ratio is maintained constant. The coolant is water.

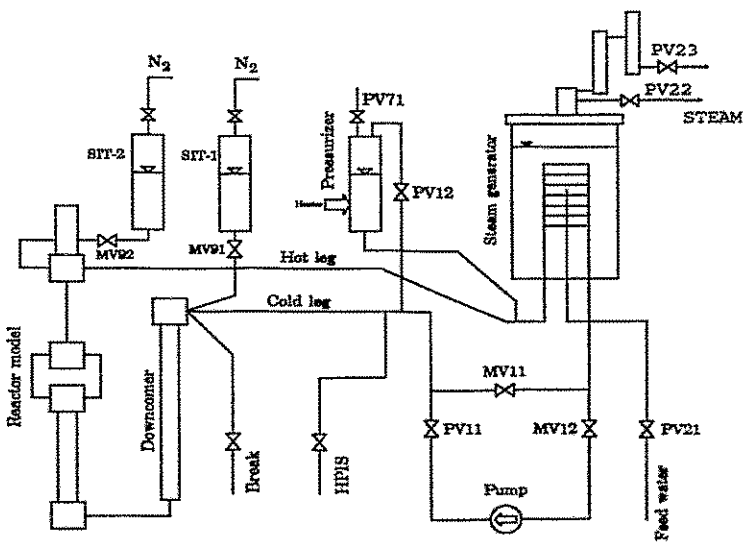

Fig. 2.1: Flow diagram of PMK-2 facility

A flow diagram of the PMK-2 is presented in Fig. 2.1. The core model with an electrically heated 19-rod bundle and the steam generator (SG) model are presented in Figs. 2.2 and 2.3, respectively.

The modifications on the facility from 1990 (previous measurement) are the location of the pressurizer surge line and the improved data aquisition system.

The measured parameters are given in Table 2.1 and their locations can be seen in Figs. 2.6-2.10.

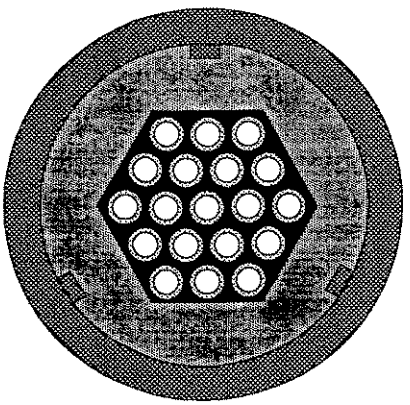

Fig. 2.2: Core model (cross section)

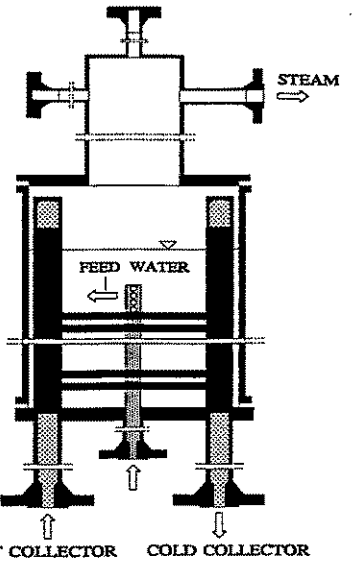

Fig. 2.3: Steam generator model

During the experiment needle shaped conductivity probe devices by RC. Rossendorf were applied. The needle shaped conductivity probes are local void fraction sensors. Their function is based on the interruption of the electrical current between the tip of the probe and the conducting fluid by the gas fraction. The void fraction is determined by integrating the time of the gas contact divided by the measuring time [6, 7].

The isolation tips of the Rossendorf needle probes are made from sintered Aluminium Oxide (Al_2O_3) ceramic (Fig. 2.4), in order to withstand the high mechanical and corrosive loads during the test. The diameter of the tip is 0.8 mm. The locations of the needle probes at PMK-2 are given in Fig. 2.10.

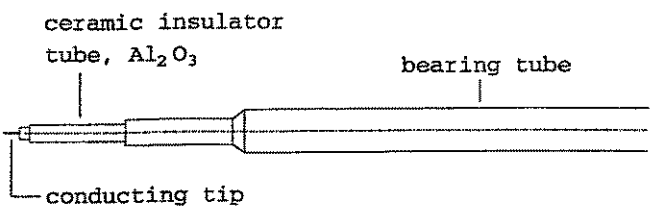

Fig. 2.4: Needle shaped conductivity probe

The measuring chain consists of a network of preamplifier modules equipped with micro-computers and a central data acquisition PC (Fig. 2.5). The modules perform a data preprocessing and control a digital interface, which is necessary to manage the high electrical disturbance levels typical for integral test facilities. In the result the time behaviour of the void fraction and the frequency of the phase changes (bubble frequency) are recorded with a sampling time of 1 sec.

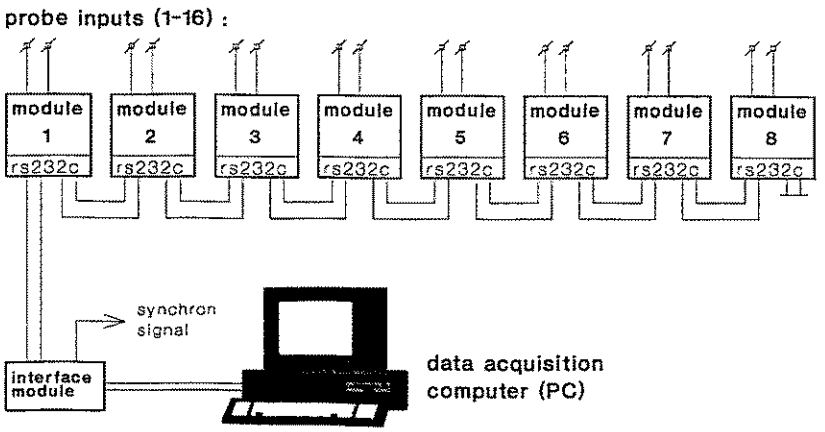

Fig. 2.5: Computerized data acquisition system for void fraction probes

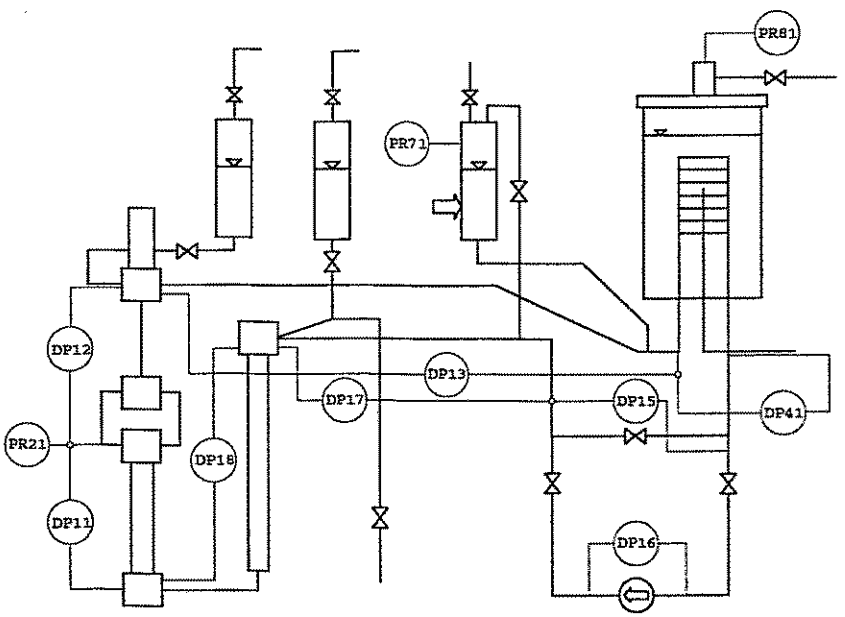

Fig. 2.6: Measurement locations (pressure, differential pressure)

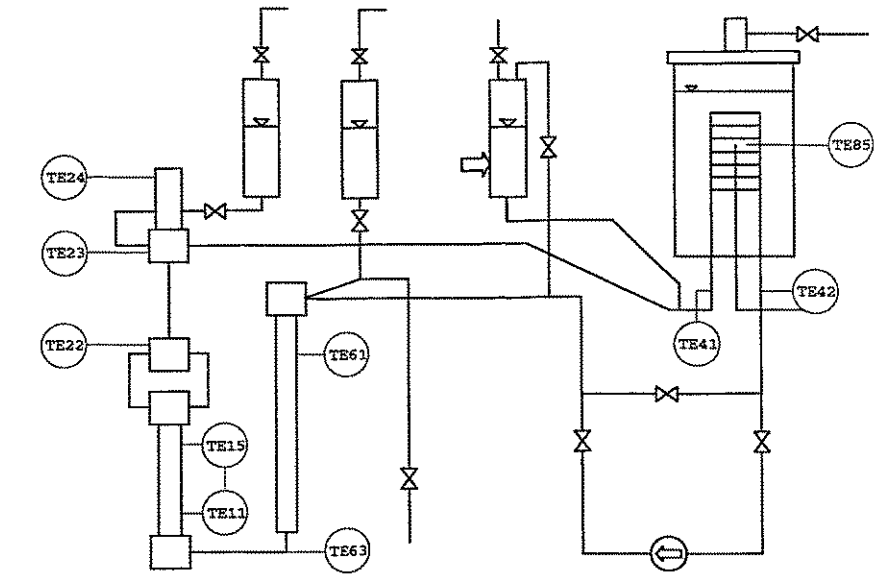

Fig. 2.7: Measurement locations (temperature)

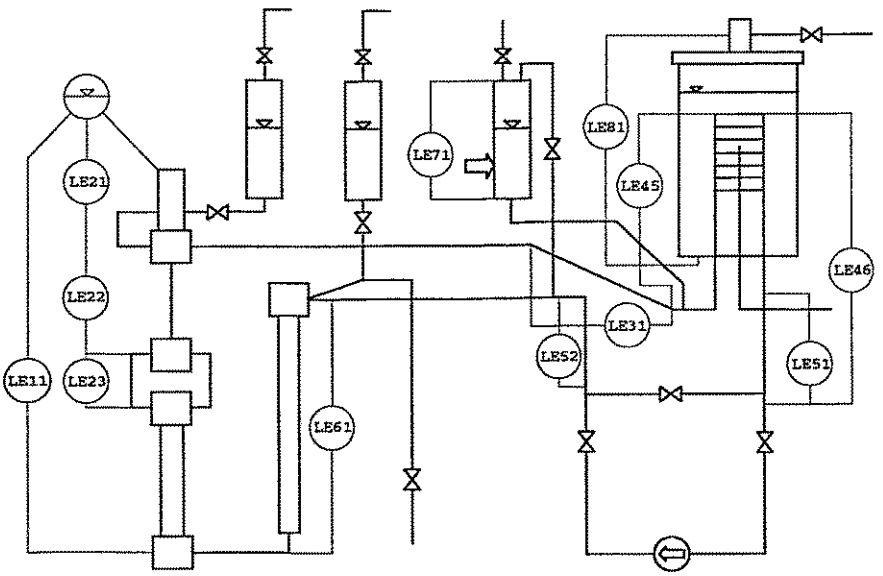

Fig. 2.8: Measurement locations (level)

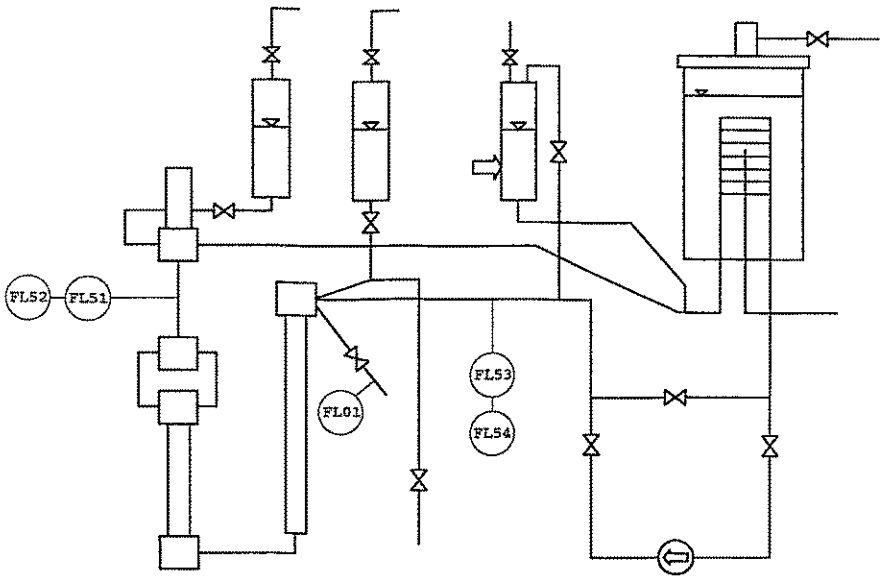

Fig. 2.9: Measurement locations (flow rate)

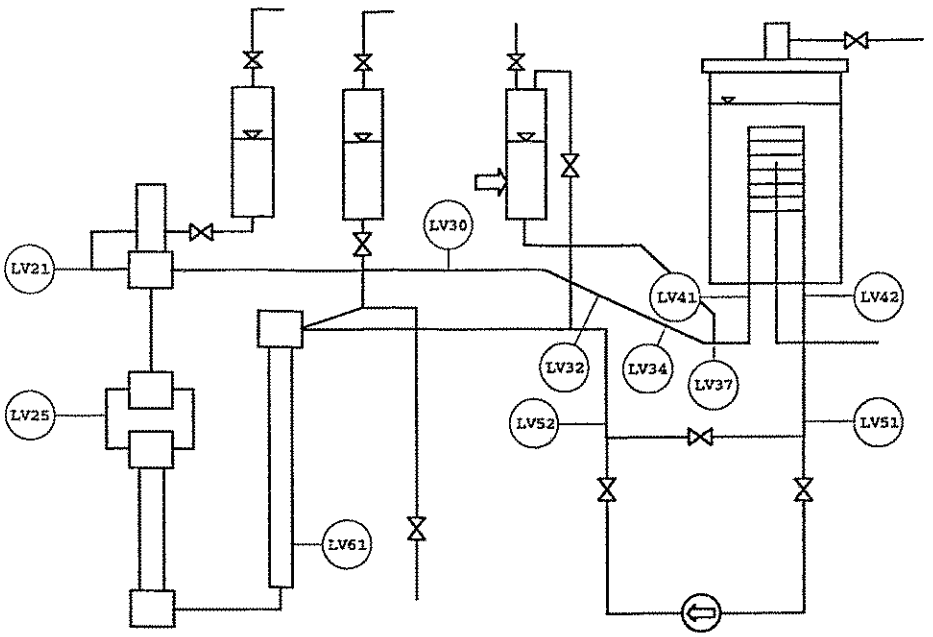

Fig.: 2.10: Measurement locations (void fraction)

Item No.	Identification	Location and type of measurement	Elevation	Measurement accuracy, less than ±	Unit
1.	TE11	Heater rod surface, termocouple,	1.494 m		
2.	TE12	" "	2.954 m		
3.	TE13	" "	3.464 m		
4.	TE14	" "	3.464 m		
5.	TE15	" "	3.464 m		
6.	TE23	Wall in upper plenum, "	6.225 m		
7.	TE62	Wall in downcomer, "	4.995 m		
8.	TE43	Heat exchanger inlet (1) "	8.163 m		
9.	TE45	" (2) "	7.591 m		
10.	TE47	" (3) "	6.385 m		
11.	TE44	" outlet (1) "	8.163 m		
12.	TE46	" (2) "	7.591 m	2 K	K
13.	TE48	" (3) "	6.385 m		
14.	TE80	Sec. water hot coll. (1) "	8.163 m		
15.	TE82	" (2) "	7.591 m		
16.	TE84	" (3) "	6.385 m		
17.	TE83	" middle (1) "	8.163 m		
18.	TE85	" (2) "	7.591 m		
19.	TE87	" (3) "	6.385 m		
20.	TE86	"cold coll. (1) "	8.163 m		
21.	TE88	" (2) "	7.591 m		
22.	TE89	" (3) "	6.385 m		
23.	TE01	break flow temperature, "	4.825 m		
24.	TE22	Upper plenum temperature, Pt resistance	4.644 m	1 K	K
25.	TE24	" "	8.375 m	"	K
26.	TE60	Coolant pump inlet, "	3.525 m	"	K

Table 2.1: Identification of measurement locations

Item No.	Identification	Location and type of measurement	Elevation	Measurement accuracy, less than ±	Unit
27.	TE61	Coolant downcomer inlet, Pt resistance	4.520 m	1 K	K
28.	TE63	Coolant at core inlet, "	0.190 m	"	K
29.	TE41	SG primary coolant inlet, "	5.995 m	"	K
30.	TE42	SG primary coolant outlet, "	5.995 m	"	K
31.	PR01	Back pressure behind break simulator	4.825 m		kPa
32.	PR21	Upper plenum	3.754 m	0.05 MPa	MPa
33.	PR71	Pressurizer pressure	10.077 m	0.05 MPa	MPa
34.	PR81	SG secondary	11.212 m	0.02 MPa	MPa
35.	DP11	Core	0.190/3.754 m	1 kPa	kPa
36.	DP12	DP between 1 and 8	3.754/6.225 m	1 kPa	kPa
37.	DP13	DP between 1 and 2	5.995/6.225 m	1 kPa	kPa
38.	DP15	DP between 4 and 5	2.725/3.525 m	1 kPa	kPa
39.	DP16	Pump DP between 4 and 5	-0.318/0.382 m	1 kPa	kPa
40.	DP17	Pump DP between 5 and 6	3.525/4.664 m	1 kPa	kPa
41.	DP18	Pump DP between 6 and 7	4.664/0.190 m	1 kPa	kPa
42.	DP41	SG primary	5.995/5.995 m	1 kPa	kPa
43.	LE11	Reactor model	0.190/9.220 m		m
44.	LE21	Upper plenum, DP	5.504/9.220 m	4×10^{-2} m	m
45.	LE22	Upper plenum, impedance probe	4.664/5.504 m	5×10^{-2} m	m
46.	LE23	Upper plenum part 1.	3.754/4.664 m	5×10^{-2} m	m
47.	LE31	Hot leg loop seal, DP (reactor side)	4.802/6.080 m	1.5×10^{-2} m	m
48.	LE45	SG primary, hot leg, DP	4.802/8.445 m	3×10^{-2} m	m
49.	LE46	SG primary, cold leg, DP	2.725/8.445 m	3×10^{-2} m	m
50.	LE51	Cold leg part 1, DP	2.725/5.995 m	3×10^{-2} m	m
51.	LE52	Cold leg pressure drop, reactor side	3.525/4.995 m	1.5×10^{-2} m	m
52.	LE60	Downcomer head, DP	4.354/4.995 m	"	m

Table 2.1

Item No.	Identification	Location and type of measurement	Elevation	Measurement accuracy, less than ±	Unit
53.	LE61	Downcomer, DP	0.190/4.995 m	$5x10^{-2}$ m	m
54.	LE71	Pressurizer, DP	7.95/10.077 m	$2x10^{-2}$ m	m
55.	LE72	Pressurizer surge line, DP	6.025/7.950 m	"	m
56.	LE81	SG secondary, DP	6.58/11.212 m	$5x10^{-2}$ m	m
57.	FL51	Core outlet, normal, venturi	5.504 m	0.06 kg/s	kg/s
58.	FL52	Core outlet, low flow, venturi	5.504 m	0.02 kg/s	kg/s
59.	FL53	Cold leg, normal, venturi	4.825 m	0.06 kg/s	kg/s
60.	FL54	Cold leg, low flow, venturi	4.825 m	0.02 kg/s	kg/s
61.	FL01	Break flow, turbine	4.025 m		kg/s
61.	FL81	Feed water flow, venturi	4.990 m	0.02 kg/s	kg/s
63.	MA01	Total mass leaked through break, DP	-	1.0 kg	kg
64.	DE21	Upper plenum, γ attenuation	5.700 m	-	-
65.	PW01	Electrical power		3.0 kW	kW
66.	LV21	Local void in upper plenum, void-probe	6.225 m		
67.	LV25	" " "			
68.	LV30	Local void in hot leg, "	6.225 m		
69.	LV32	Local void in hot leg loop seal, "	5.400 m		
70.	LV34	Local void in hot leg loop seal, "			
71.	LV37	Local void in hot leg loop seal, "	4.802 m		
72.	LV41	" in SG hot collector, "	5.995 m		
73.	LV42	" in SG cold collector, "	5.995 m		
74.	LV51	" in cold leg, "	3.525 m		
75.	LV52	" " "	3.525 m		
76.	LV61	Local void in downcomer, "			

Table 2.1

3. Experiment description

The test is characterized as follows. The break nozzle has a diameter of 1mm (modelling a 1% break in the Paks NPP) and is located on the upper head of the downcomer. The modelling of the HPIS flow corresponds to the case when only one of the three systems is available. The unavailability of SIT system is assumed. Transient is initiated by opening valve MV31. The secondary side is isolated after transient initiation by closing valves PV21 and PV22.

The initial steady state conditions for the test are presented in Chapter 3.1 (for the abbreviations, see Fig. 2.6-2.10). The sequence of events during the course of transient is summarized in Chapter 3.2. Accuracy is given in Table 2.1.

3.1 Measured initial conditions

For the comparison, the values of the previous measurement (1990) are included.

Primary circuit	**1990**	**1994**	
- System pressure (PR21)	12.39	12.43	MPa
- Loop flow (FL53)	4.65	5.10	kg/s
- Core inlet temperature (TE63)	539.2	536.4	K
- Power	612.6	658.0	kW
- Coolant level in PRZ (LE71)	9.07	9.02	m

Secondary circuit	**1990**	**1994**	
- Pressure (PR81)	4.73	4.51	MPa
- Feedwater flow (FL81)	0.374	0.348	kg/s
- Feedwater temperature (TE81)	493.0	496.2	K
- Coolant level in SG (LE81)	7.83	7.85	m

3.2 Sequence of events

	1990	1994	
- Break valve starts to open	0.0	0.0	s
- SCRAM is initiated at	11.55 (72	11.59 65	MPa s)
- Pump coastdown	11.21 (81	11.07 74	MPa s)
- HPIS flow is initiated at Time delay is 37 s , flow rate is 0.014 kg/s.	11.55 (72	11.59 65	MPa s)
- SG relief valve opens at	5.26 (15	5.39 41	MPa s)
- SG relief valve closes at	4.89 (141	4.96 150	MPa s)
- Test was terminated at	3638	3998	s

4. Results and discussion

The measured parameters selected for this report are given in Figs. 4.1 - 4.22. These figures contain the calculation results of the RELAP5 and ATHLET codes. For the identification Table 2.1 should be used.

The time variation of the system pressure (PR21) is presented in Fig. 4.8. Opening the break results in a fast decrease in pressure which is characteristic for the subcooled blowdown. It can be seen, however, that there is a change in the slope of the pressure decrease. The reasons are as follows: the SG relief valve (PV23) opens at 41 s when the secondary pressure is 5.39 MPa. However, as a consequence of the fact that the full power is on the core model until 65 s, the pressure increase lasts until 74 s, when there is a sharp drop on the pressure curve as shown in Fig. 4.9. As a consequence the primary pressure decrease is also accelerated and continuously drops to 6.2 MPa at 170 s, when the coolant temperature in the upper plenum reaches the saturation temperature (see Fig. 4.4).

The pump coastdown is started at 71 s. The sink in the flow curve (see Fig. 4.20) is a consequence of the valve-off procedure (PV11 closes, MV11 opens and MV12 closes). After the pump bypass is valved off, the two-phase natural circulation is being developed in the loop. As shown in the Fig. 4.20, there is a steady state flow in the loop.

The pressurizer is emptied at 180 s (see Fig. 4.11). The HPIS flow is initiated at a system pressure of 11.59 MPa (65 s). Taking into account the time delay the HPIS flow appears in the loop at 102 s.

Due to the interaction between primary and secondary sides the decrease in system pressure is slow. The SG relief valve is closed at 150 s (4.96 MPa). The primary pressure equals secondary pressure at 1710 s.

The system pressure shows a local maximum at a transient time of 760 s. This is the effect of the hot leg loop seal. It is shown in Fig. 4.12, that hot leg loop seal reactor side starts to empty at 620 s. That the level is sufficiently low at 760 s to allow the steam generated in the core to pass the loop seal.

Close after the level in the loop seal had reached the lowest point significant oscillation of the levels in the reactor and in the hot collector of the steam generator were observed. The signals of the differential pressure transducers are verified by the void fraction probes. The probes indicated void fraction oscillations, which are in excellent agreement with the behaviour of the levels (Fig. 4.23). The loop seal clearing occurred at t=750 s, when the level in the inclined part of the hot leg (LE31) reached the bottom of the loop seal. After a few seconds the first steam bubbles were indicated by probe LV41 at the inlet of the hot collector. At first, the steam volume pushed into the collector led to an increase of the flow rate in the circuit between t=750 and 785 s (Fig. 4.24, FL54). At the same time condensation started in the steam generator and the pressure began to decrease.

As a result of the increased flow rate the level in the reactor model (LE11) grew up and a two-phase flow was reestablished at the reactor outlet. This was indicated by probe LV21. This caused a partially refilling of the loop seal shown by probe LV41 and level LE45 in the period between t=785 and 800 s. The interrupted supply of steam together with the continuing

condensation caused a volume sink in the steam generator. As the result the flow in the circuit reversed or at least stagnated (see FL54). The reactor level decreased in this period causing an increasing void fraction at the reactor outlet, so that the loop seal was cleared again.

When the condensation had stopped, a pressure increase was observed until the next occurrence of steam in the hot collector. The shape of the pressure slope has an additional effect on the mixture level in the reactor vessel. The mixture level is growing faster than the collapsed level indicated by LE11 if the pressure is falling. Because of condensation effects, in the opposite case the mixture level approaches the collapsed level, when the pressure is rising.

The described process was repeating periodically until the coolant mass had been decreased to such a degree that the level was no more able to reach the elevation of the reactor outlet. This state was established at about t=1000 s. The period of the oscillations was approximately 18-19 s.

The statement concerning the hot leg loop seal clearing is supported by the SG inlet temperature (Fig. 4.5), the coolant temperature in the upper plenum (Fig. 4.4) and in the core inlet temperature (Fig. 4.3). The effect can also be seen in the fuel rod temperature as shown in Fig. 4.1.

From the pump coastdown, until 1380 s the flow in the steam generator is practically zero. As shown in Fig. 4.19, however, the pressure drop on the SG is increasing and reaches about 2.4-2.5 kPa. It means that there is a positive flow in the steam generator. This is evidenced by the SG outlet temperature presented in Fig. 4.6. The sharp temperature increase is a consequence of the hot fluid coming from the hot collector.

The most interesting and most important phenomena are connected with the cold leg loop seal behaviour between the time interval of 1500-2000 s.

As shown in Fig. 4.10 the reactor level has an absolute minimum at 1775 s and the value is 2.5 m. This deep sink is a consequence of the cold leg loop seal. As a result of the effect of the cold leg loop seal there is an extended dryout in the core (see Fig. 4.2). The rapid temperature increase starts at 1737 s, reaches a maximum value of 690 K at 1835 s, then due to the rewetting the temperature sharply drops to the saturation temperature at 1878 s. The coolant collapsed level at 1737 s, when the temperature excursion is started, is 2.92 m, and the level, when the fuel rod surface temperature drops to about the saturation temperature of the coolant, is 3.11 m. The phenomena are supported by the variation of the coolant level in the cold leg.

The level in the cold leg collector drops to 3.78 m at 1786 s. The clearing of the cold leg loop seal reactor side is started at 1806 s. The loop seal is completly cleared at 1858 s. This is evidenced by coolant temperature in Fig. 4.7. The sharp increase of the temperature corresponds to the opening of the seal. Level changes during the loop seal clearing phenomena are presented in Fig. 4.10. The loop seal behaviour can also be observed in the pressure drop of the core (see Fig. 4.18).

After the cold leg loop seal clearing, practically there is no event until the end of the measured process time.

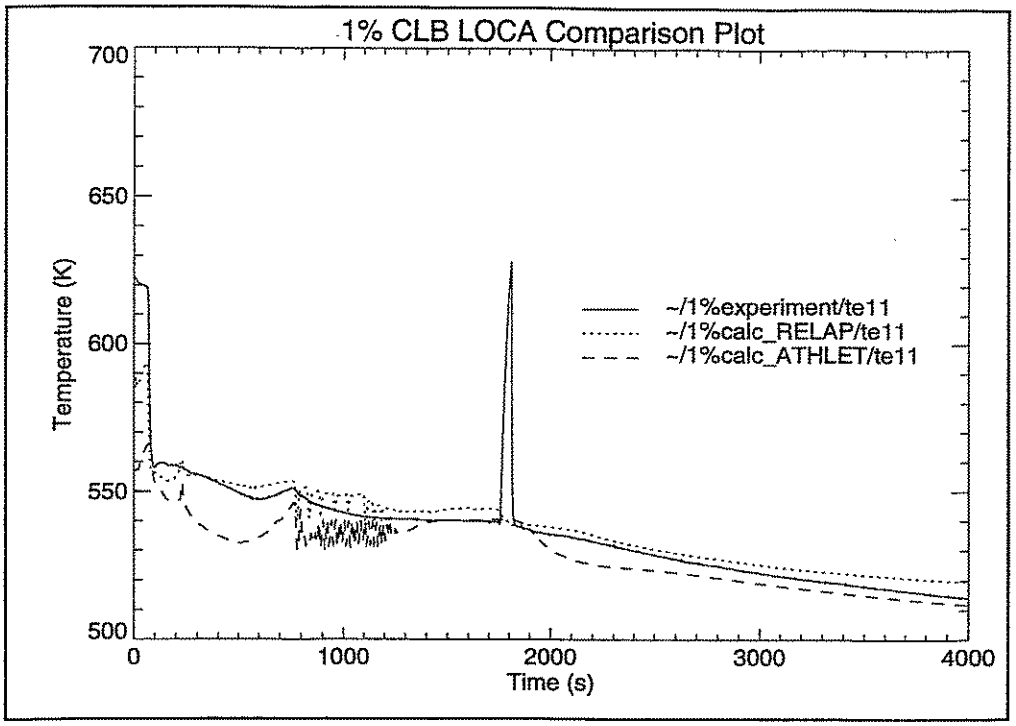
1% CLB LOCA Comparison Plot
Temperature (K)
700
650
600
550
500
0
1000
2000
3000
4000
Time (s)
~/1%experiment/te11
~/1%calc_RELAP/te11
~/1%calc_ATHLET/te11

Fig 4.1

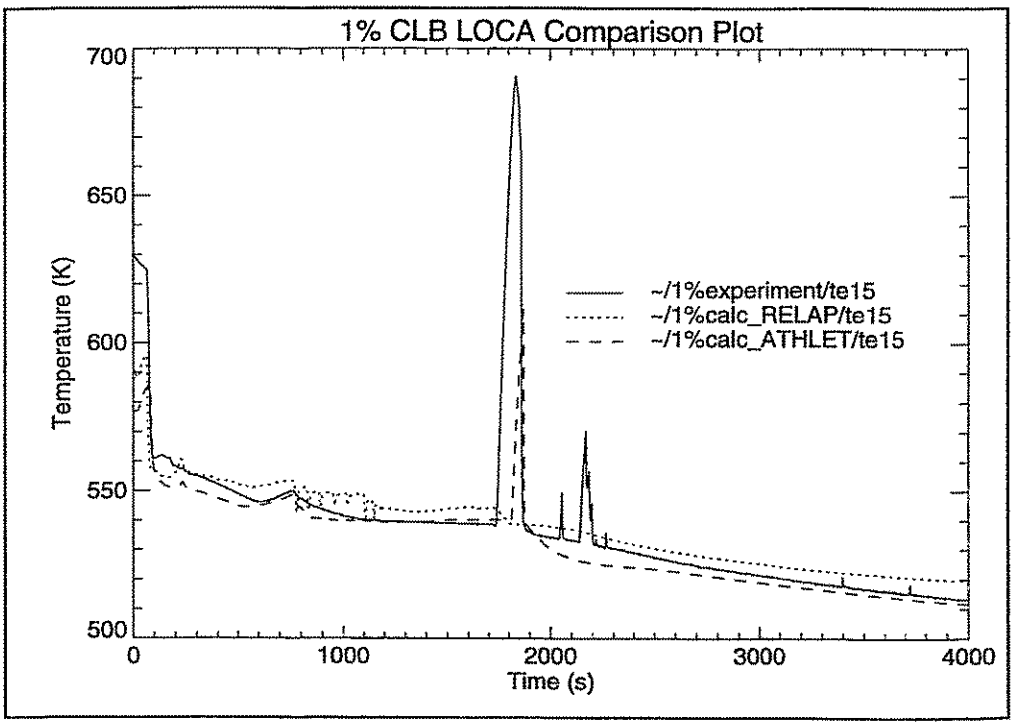
1% CLB LOCA Comparison Plot
Temperature (K)
700
650
600
550
500
0
1000
2000
3000
4000
Time (s)
~/1%experiment/te15
~/1%calc_RELAP/te15
~/1%calc_ATHLET/te15

Fig. 4.2

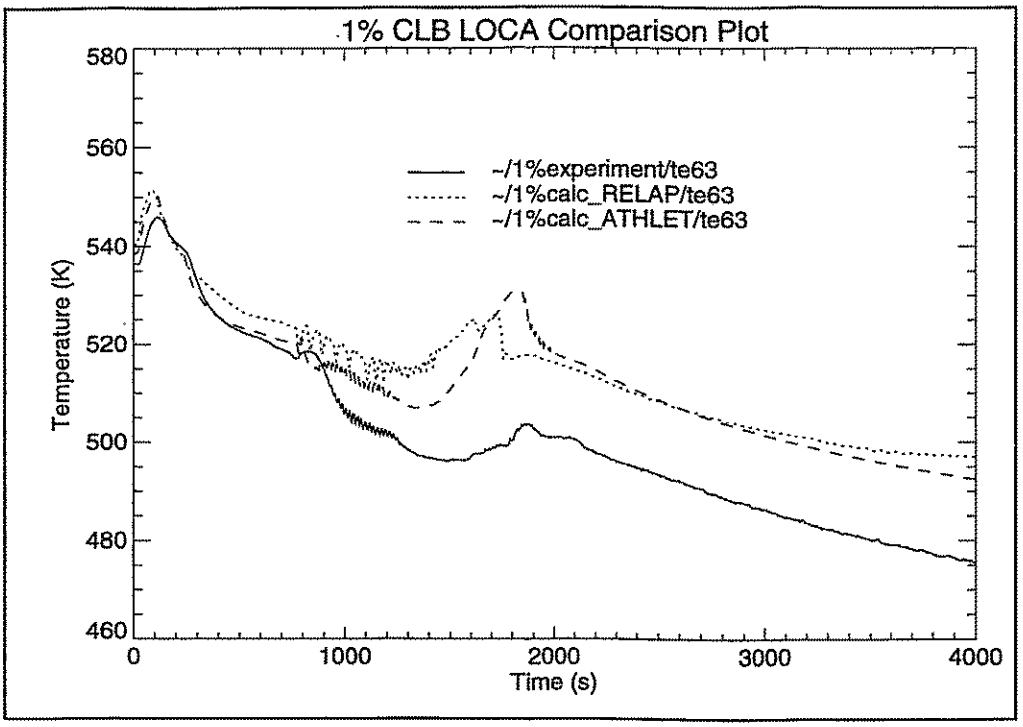
1% CLB LOCA Comparison Plot
~/1%experiment/te63
~/1%calc_RELAP/te63
~/1%calc_ATHLET/te63
Temperature (K)
Time (s)
580
560
540
520
500
480
460
0
1000
2000
3000
4000

Fig. 4.3

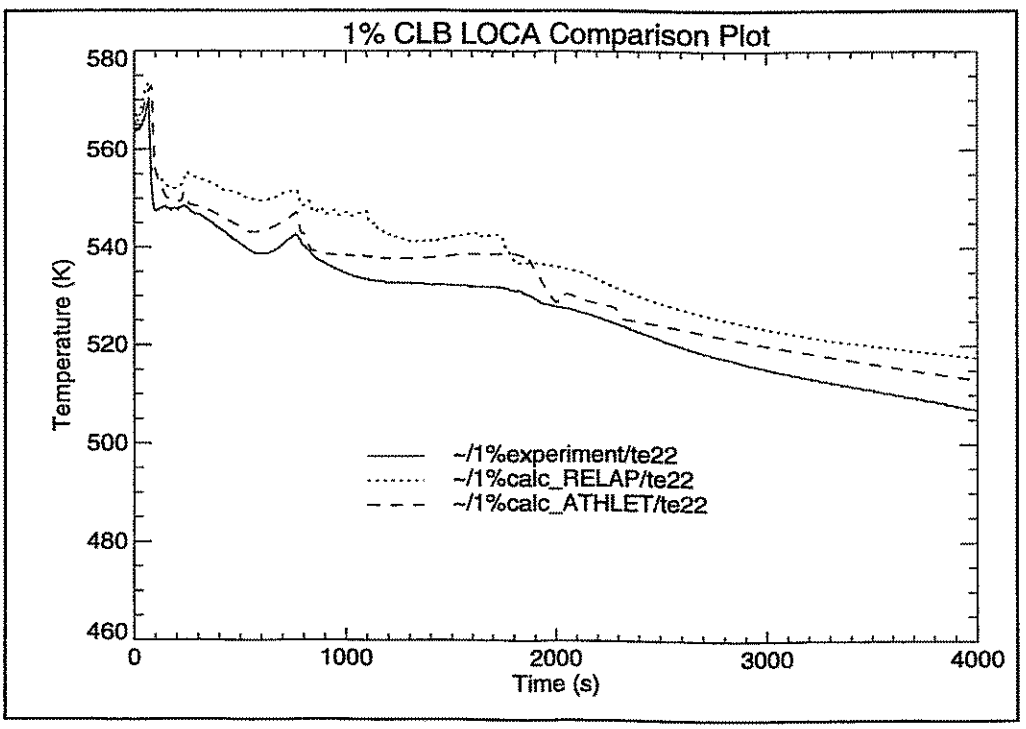
1% CLB LOCA Comparison Plot
~/1%experiment/te22
~/1%calc_RELAP/te22
~/1%calc_ATHLET/te22
Temperature (K)
Time (s)
580
560
540
520
500
480
460
0
1000
2000
3000
4000

Fig. 4.4

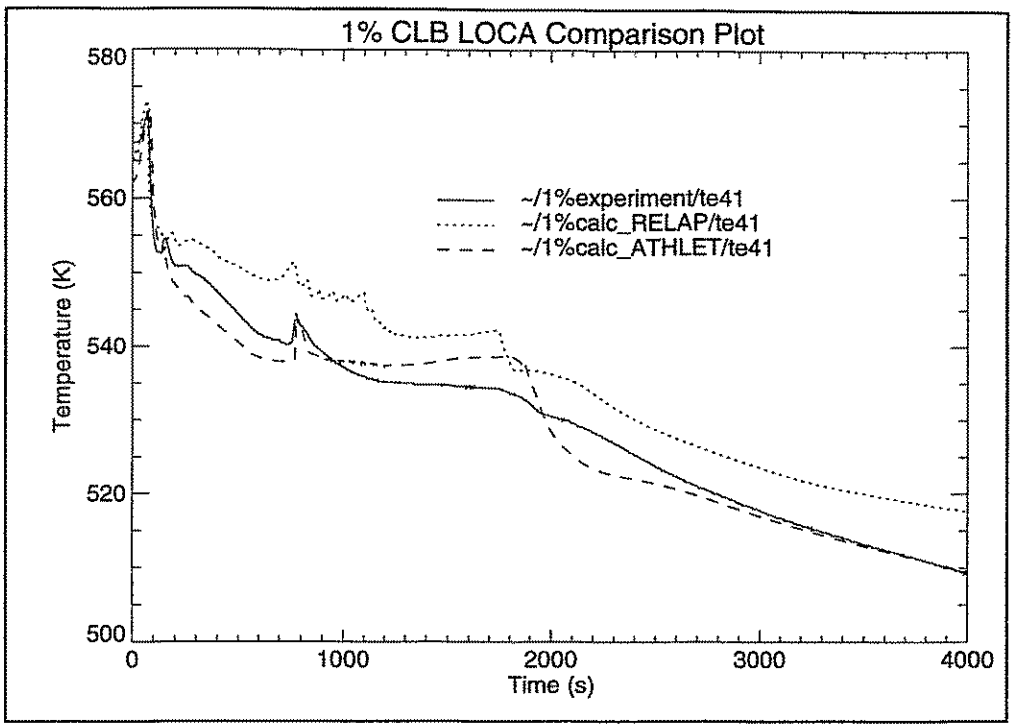
1% CLB LOCA Comparison Plot
580
560
540
520
500
Temperature (K)
0
1000
2000
3000
4000
Time (s)
~/1%experiment/te41
~/1%calc_RELAP/te41
~/1%calc_ATHLET/te41

Fig 4.5

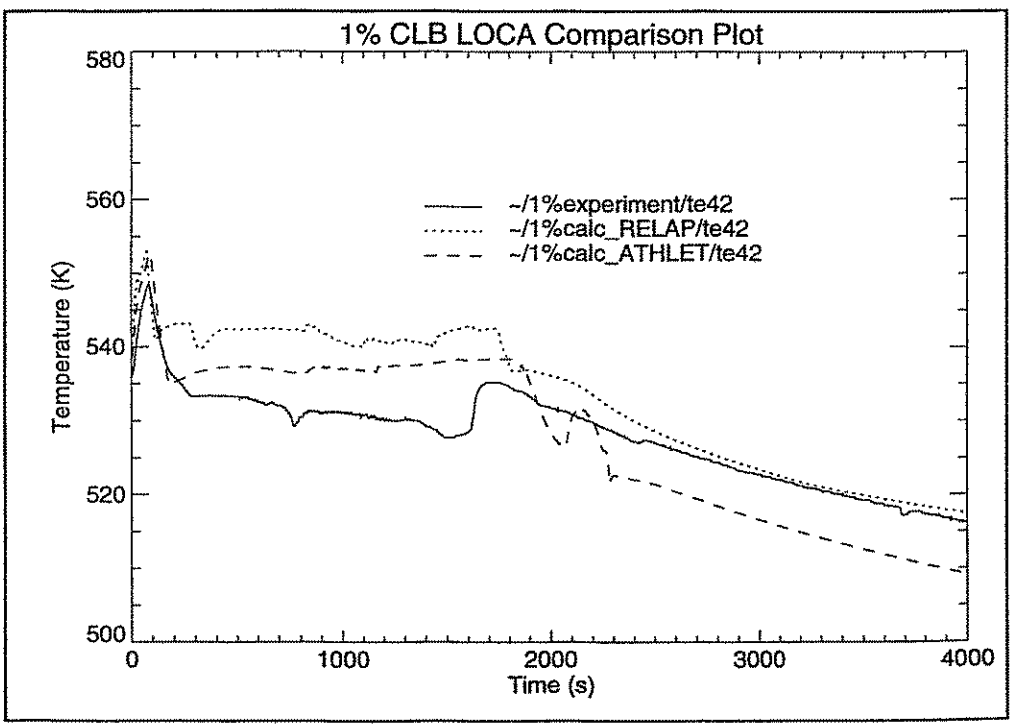
1% CLB LOCA Comparison Plot
580
560
540
520
500
Temperature (K)
0
1000
2000
3000
4000
Time (s)
~/1%experiment/te42
~/1%calc_RELAP/te42
~/1%calc_ATHLET/te42

Fig. 4.6

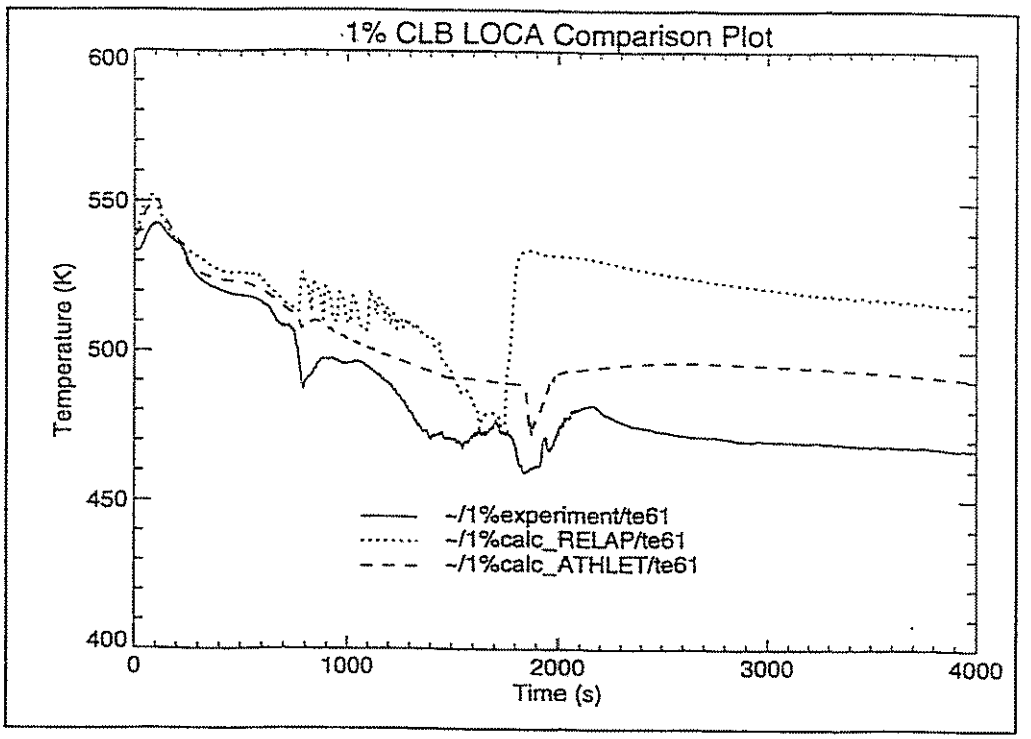
1% CLB LOCA Comparison Plot
Temperature (K)
600
550
500
450
400
0
1000
2000
3000
4000
Time (s)
~/1%experiment/te61
~/1%calc_RELAP/te61
~/1%calc_ATHLET/te61

Fig. 4.7

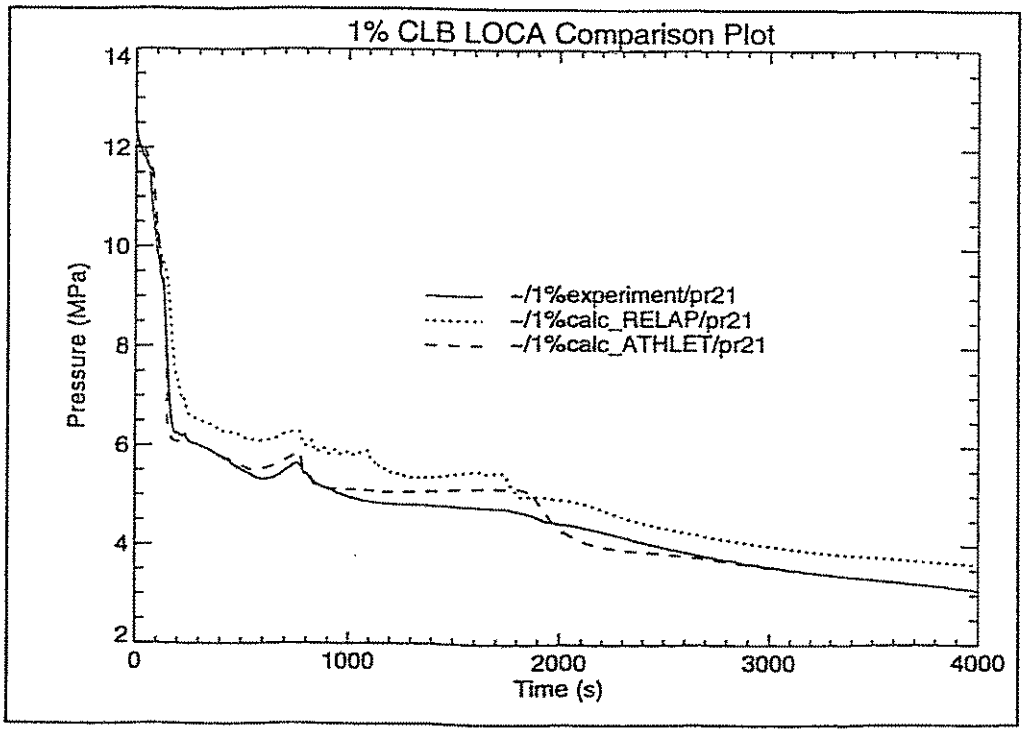
1% CLB LOCA Comparison Plot
Pressure (MPa)
14
12
10
8
6
4
2
0
1000
2000
3000
4000
Time (s)
~/1%experiment/pr21
~/1%calc_RELAP/pr21
~/1%calc_ATHLET/pr21

Fig. 4.8

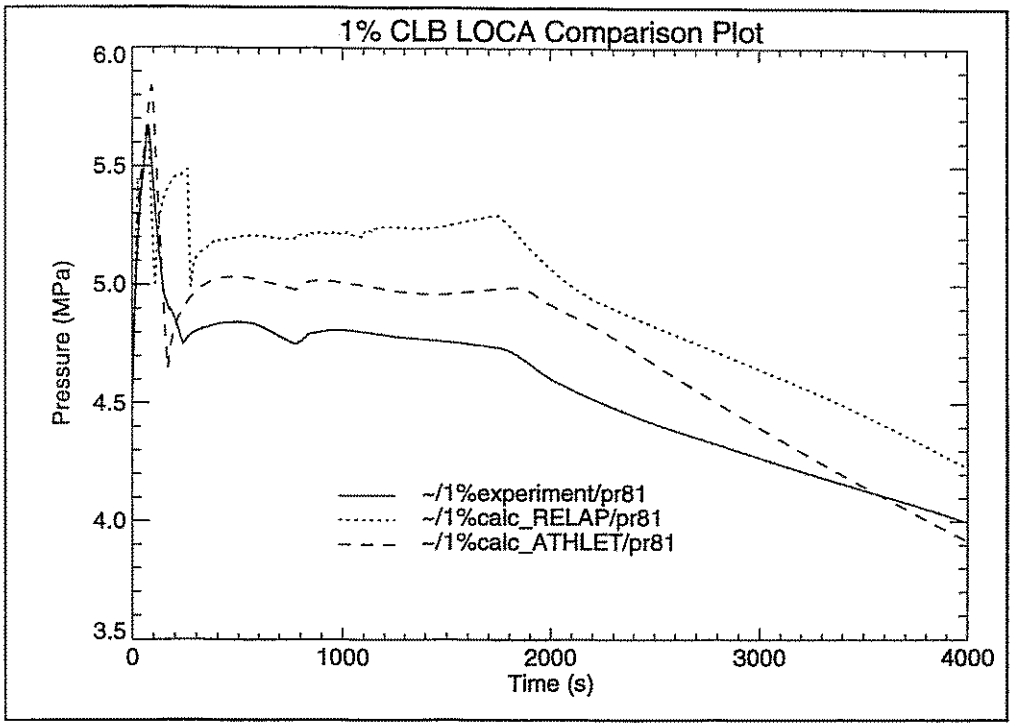

Fig 4.9

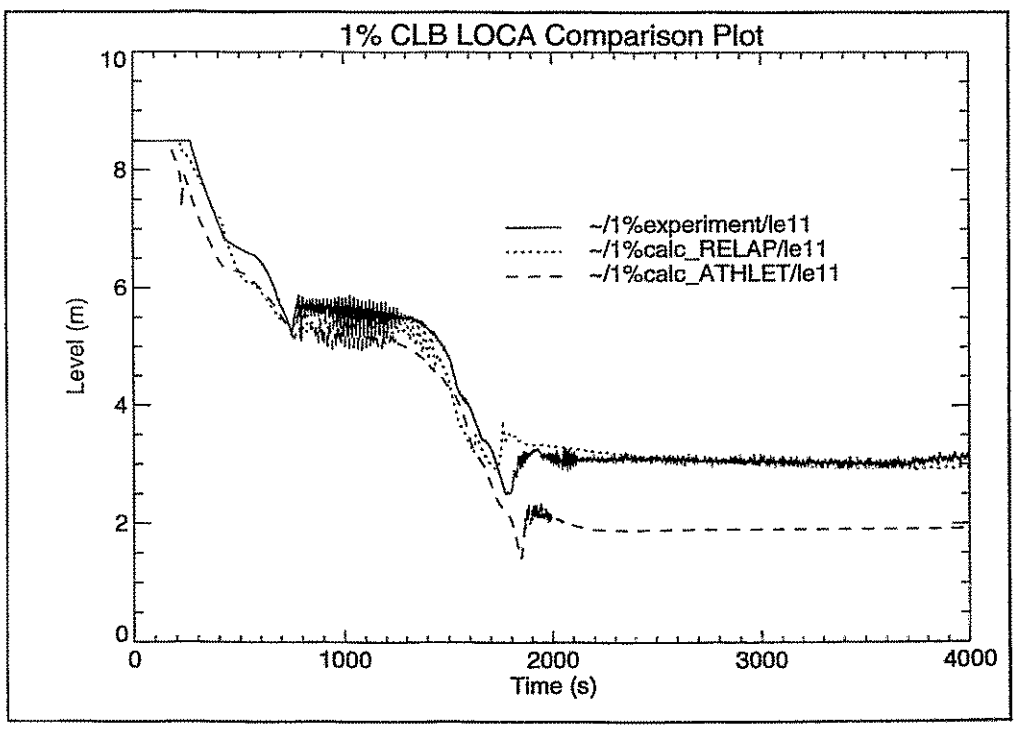

Fig. 4.10

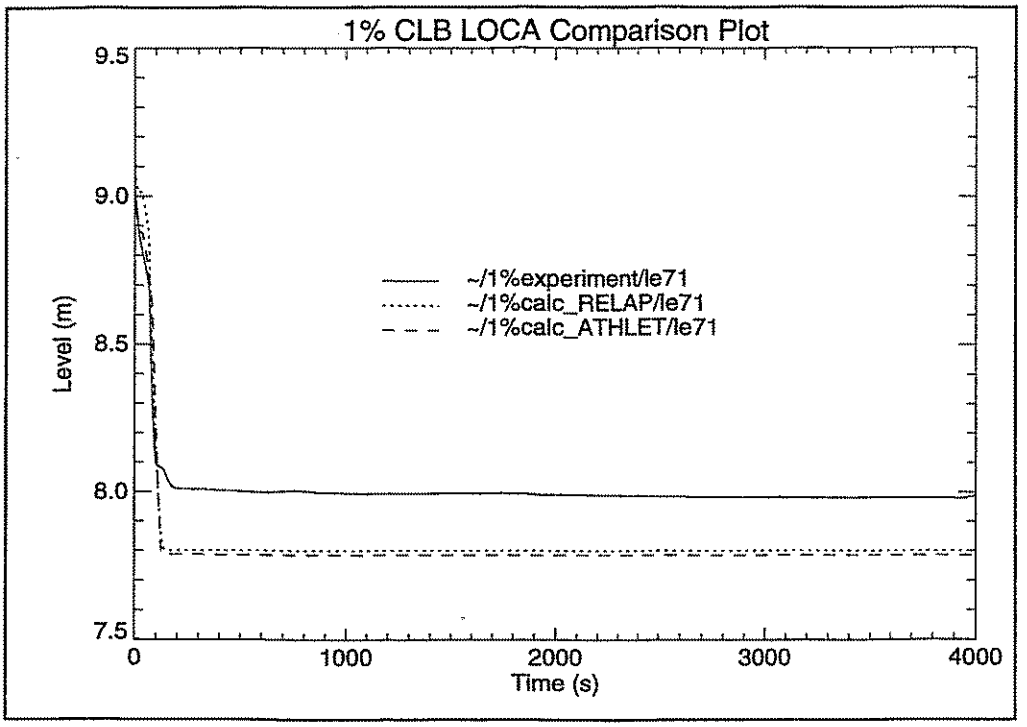

Fig. 4.11

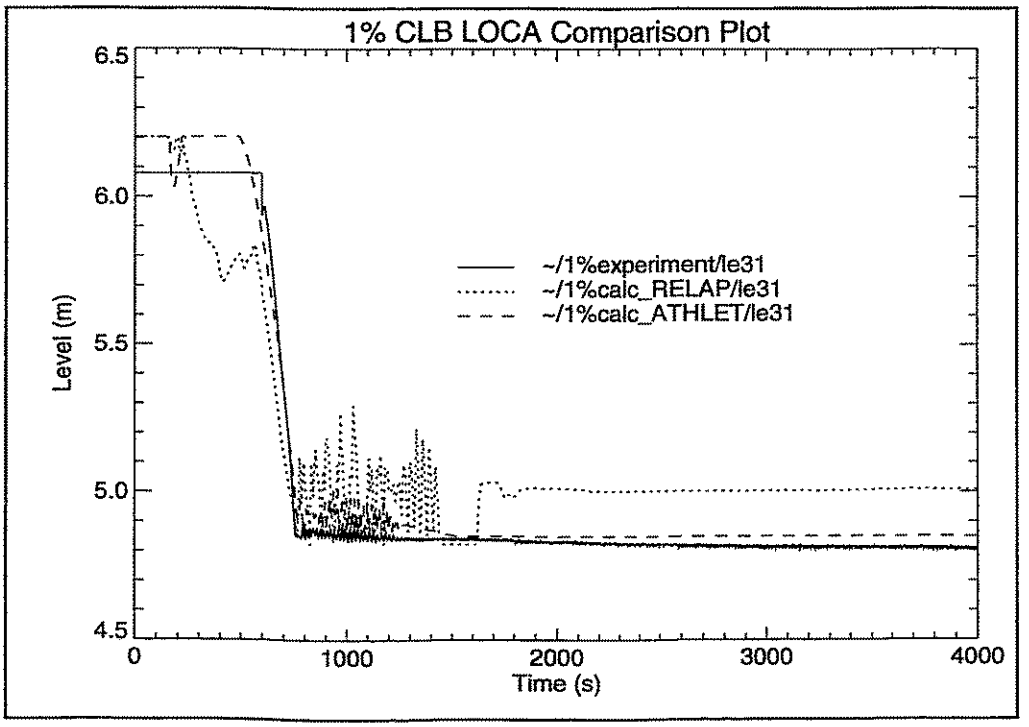

Fig. 4.12

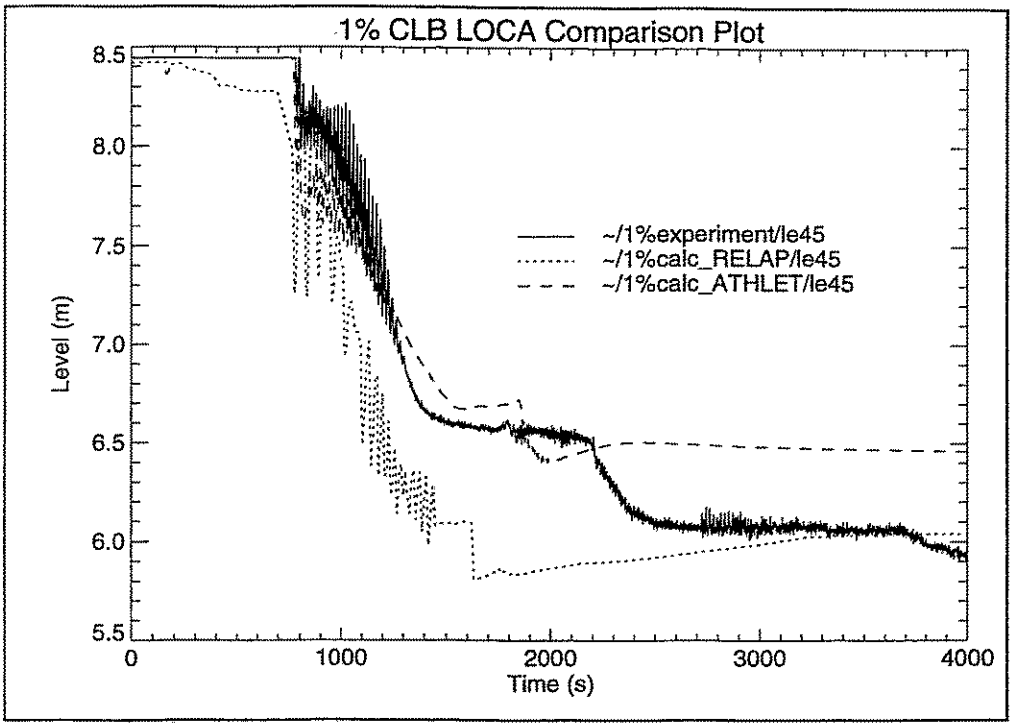

Fig 4.13

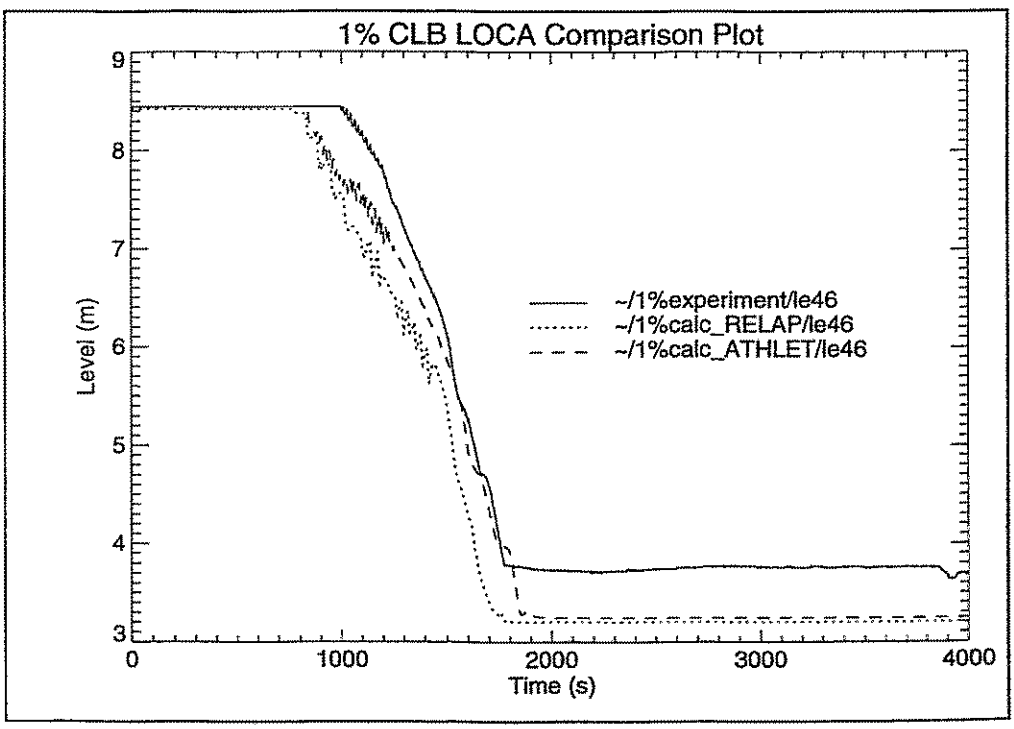

Fig. 4.14

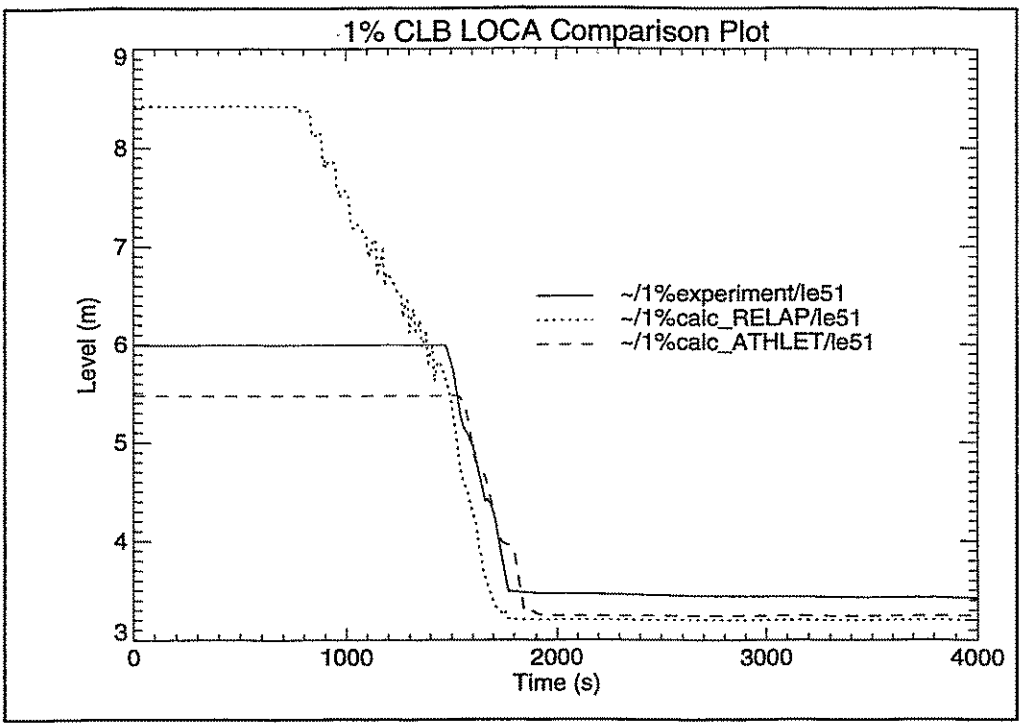

Fig. 4.15

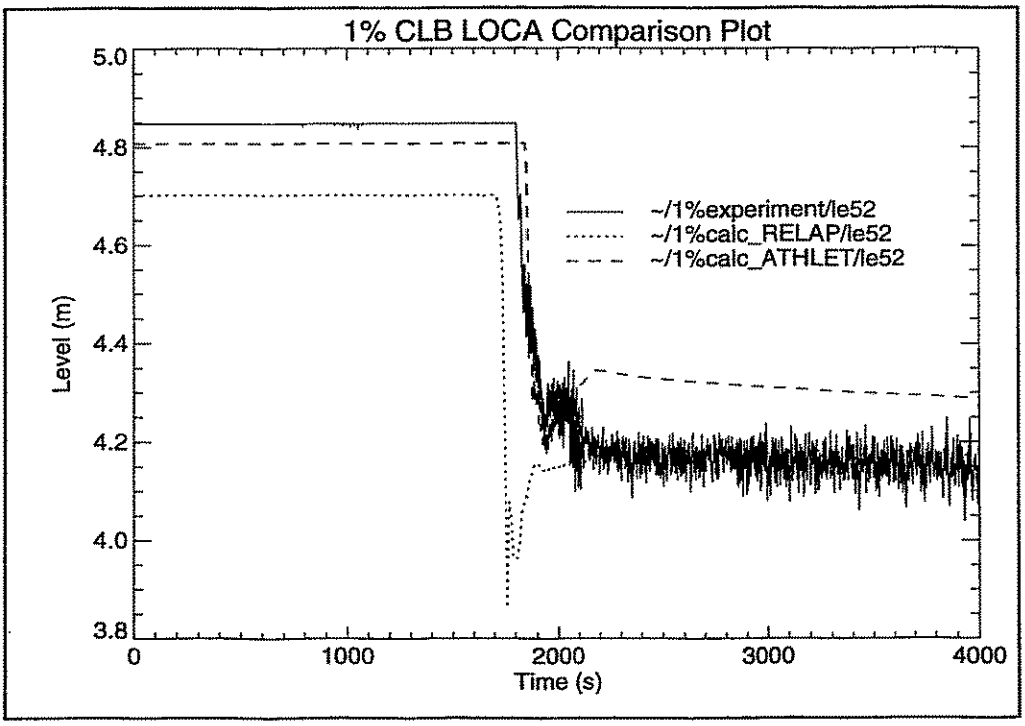

Fig. 4.16

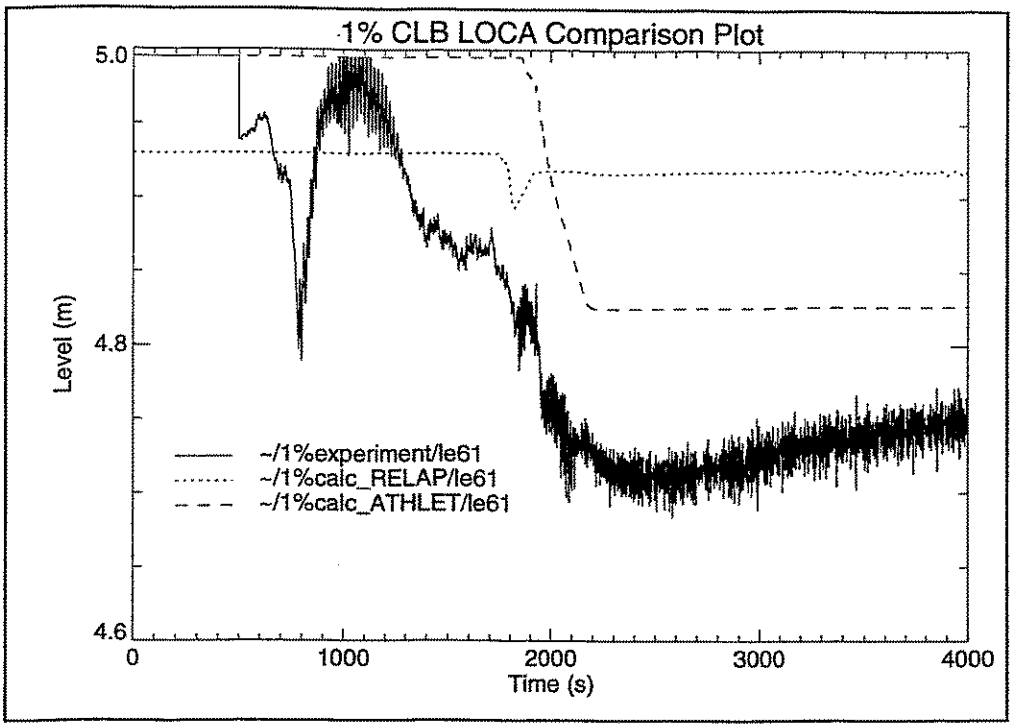

Fig. 4.17

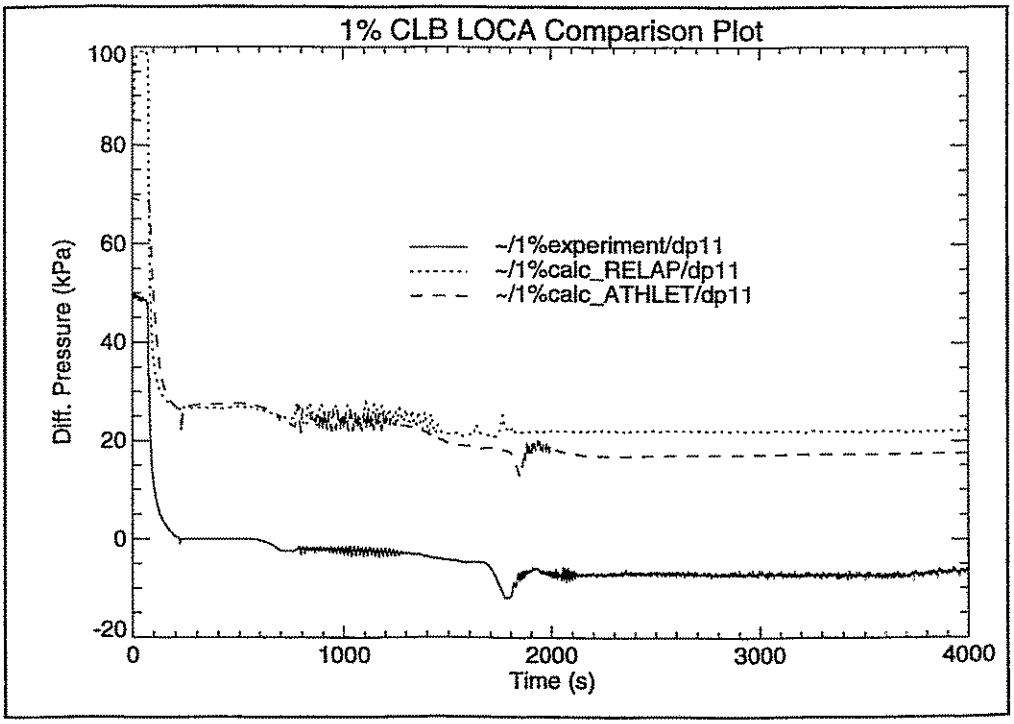

Fig. 4.18

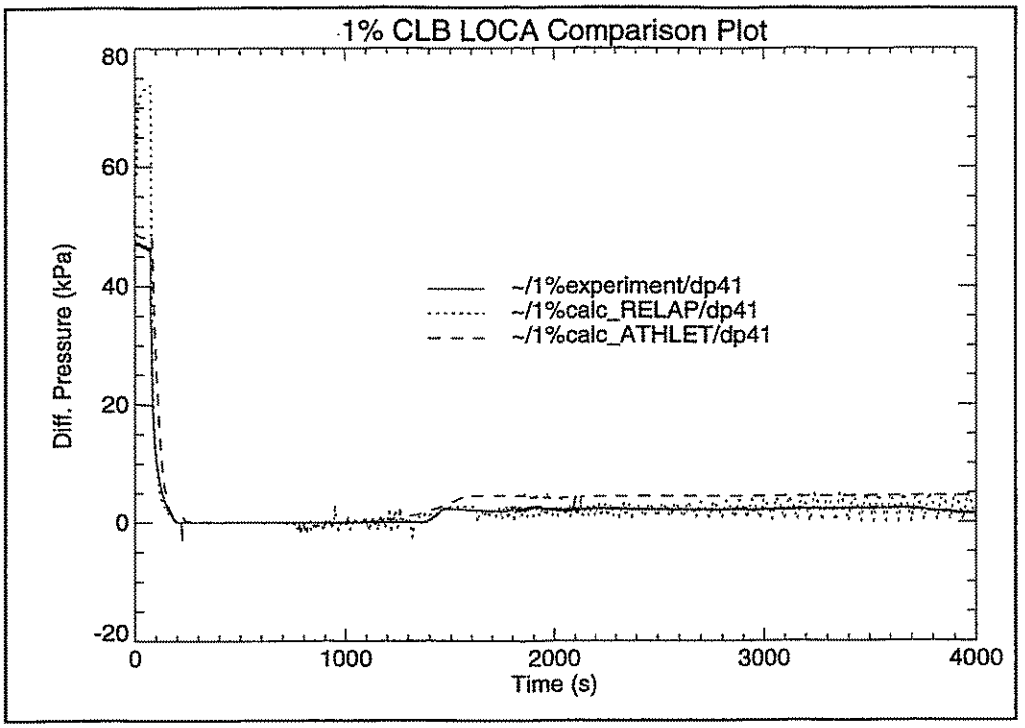

Fig. 4.19

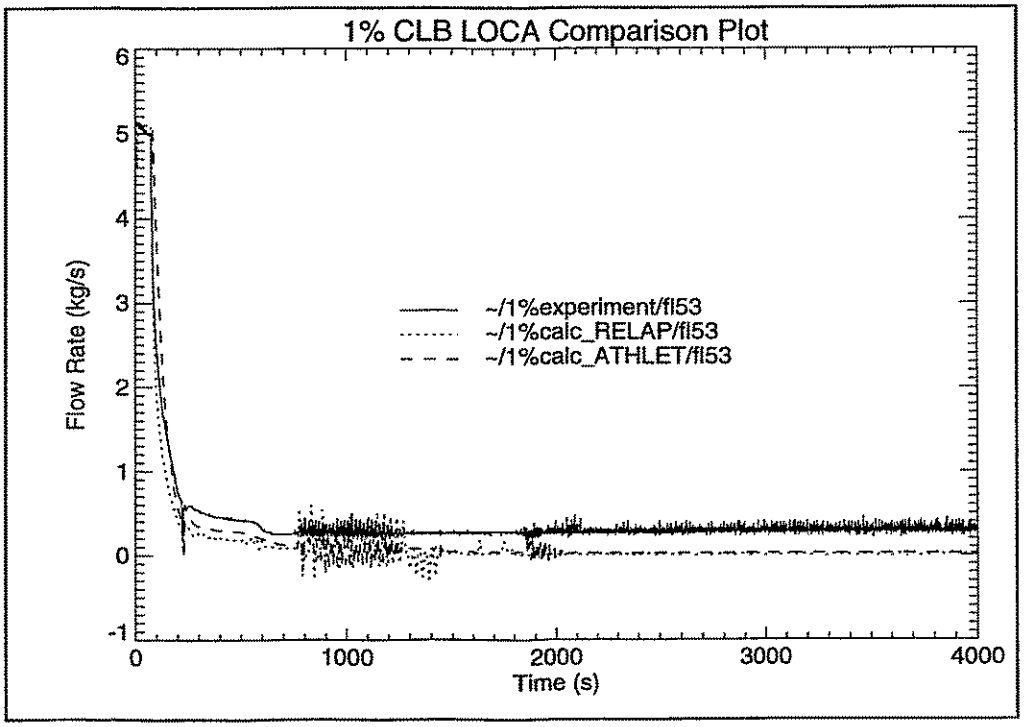

Fig. 4.20

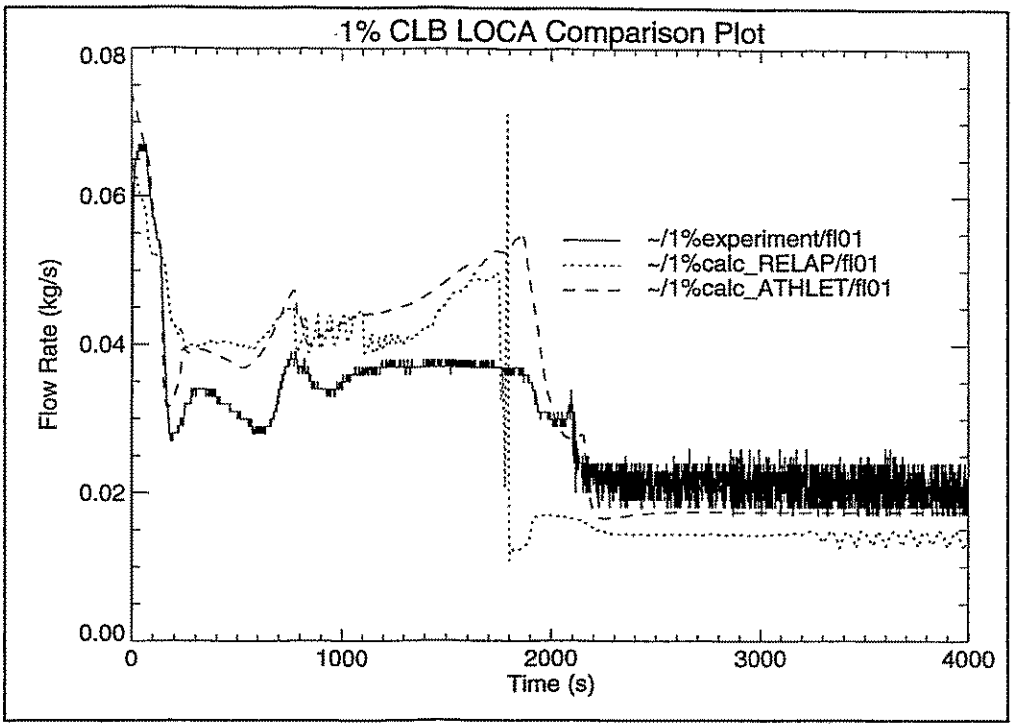

Fig 4.21

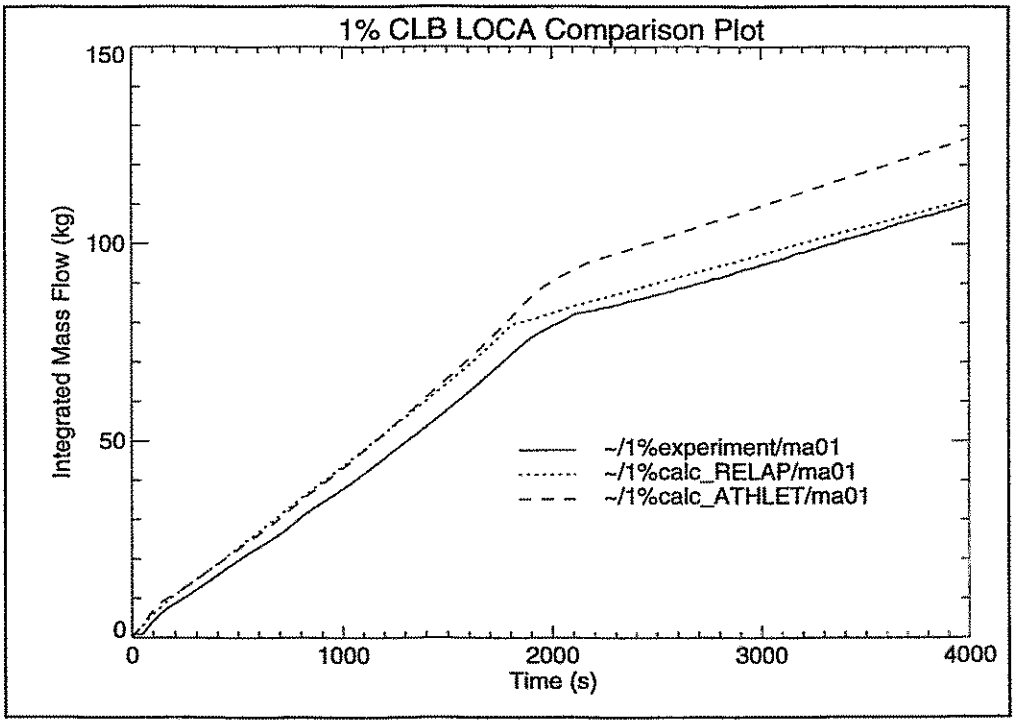

Fig. 4.22

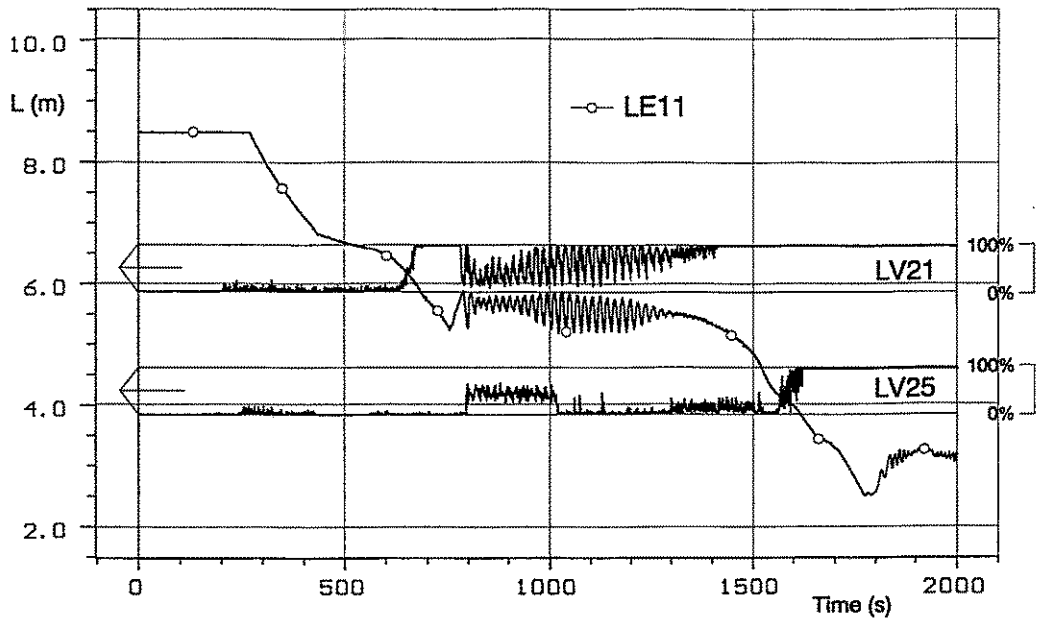

Fig. 4.23: Collapsed level (LE11) and local void fraction in the reactor model (LV)

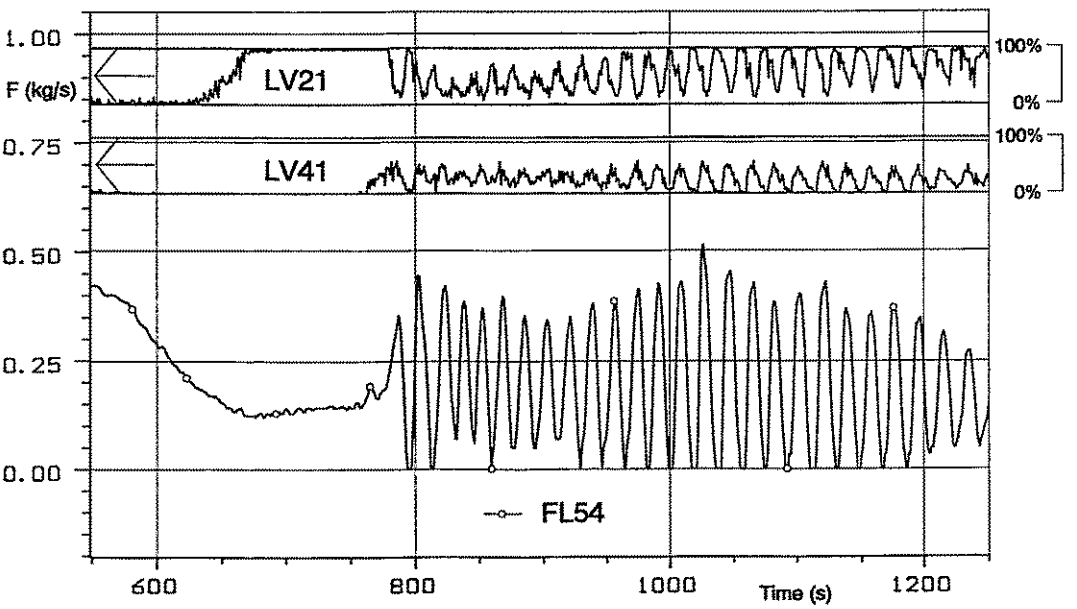

Fig. 4.24: Oscillations in flow rate (FL54) and local void fraction (LV) during the hot leg loop seal clearing

5. ATHLET calculations

At the Research Center Rossendorf post test calculations for the 1%-cold leg break experiment are performed. For the calculations the thermohydraulic code ATHLET Mod 1.1 Cycle A is used. The calculations are carried out on a Sun Workstation SPARC 10/40.

5.1 Modelling of the experiment

For modelling the thermofluid objects in most cases the four equation model of ATHLET is used (overall energy, overall momentum, liquid and vapour mass). The complete PMK-model consists of 104 control volumes, 109 junctions and 126 heat conduction volumes. The nodalization scheme is shown in Fig.5.1. In most control volumes the flooding based drift model is applied. The wall friction is considered by using the Martinelli Nelson friction model. In order to calculate the flow out of the break the one dimensional steady state critical discharge model of the ATHLET code is applied. Therefore the finite difference solution method (1DFD) is used. This is a four equation model which considers thermal nonequilibrium for one phase, whereas the other phase is kept in the state of equilibrium. For modelling the bleed valve of the steam generator secondary side the Moody model is used.

Different kind of nodalizations are tested for modelling the steam generator, e.g. the primary side is modelled by one, two or four tube bundles. Best results, however, are calculated by modelling the steam generator with two tube bundles for the primary side (including all 82 pipes of the steam generator model) and one vertical pipe for the secondary side.

The pump coast down is simulated by closing the valve PV11. For this valve the mass flow and the closing time is measured in dependence on the closing current. In order to obtain the valve characteristic the mass flow has to be show to be depended on the closing time. Therefore in the calculation a appr. linear decrease of the valve cross section during 150s is assumed. The given dependence of the pressure difference of the pump from time is considered in modelling the pump behaviour.

Before starting the transient, a steady state calculation at stationary boundary conditions is performed over a problem time of 1000 seconds. During this time the pressure of the pressurizer (PR71) is controlled by heating to compensate the heat losses of the pressurizer. This heater is switched of at the begin of the transient. The pressure of the steam generator secondary side (PR81) is controlled by the steam mass flow through valve PV22. The level of the steam generator secondary side is controlled by the feed water mass flow (FL81). During the steady state calculation the given stationary mass flow (FL53), the pressure differences and the heat losses are adjusted. For the calculation of the heat losses an insulation with an outer heat transfer coefficient of $9 W/m^2K$ is assumed. The given heat losses are established by the heat conductivity of the insulation material.

The start of calculation, the initiation of SCRAM, pump coast down and the start of high pressure injection system (HPIS) are modelled by means of special defined GCSM signals. The initiation of SCRAM, pump coast down and HPIS are controlled by the primary pressure. The time dependence of the reactor power is given in the table section of the ATHLET input dataset. As shown in the nodalization scheme the HPIS is modelled as a fill with a constant flow rate. Other emergency cooling systems in case of this experiment are not available.

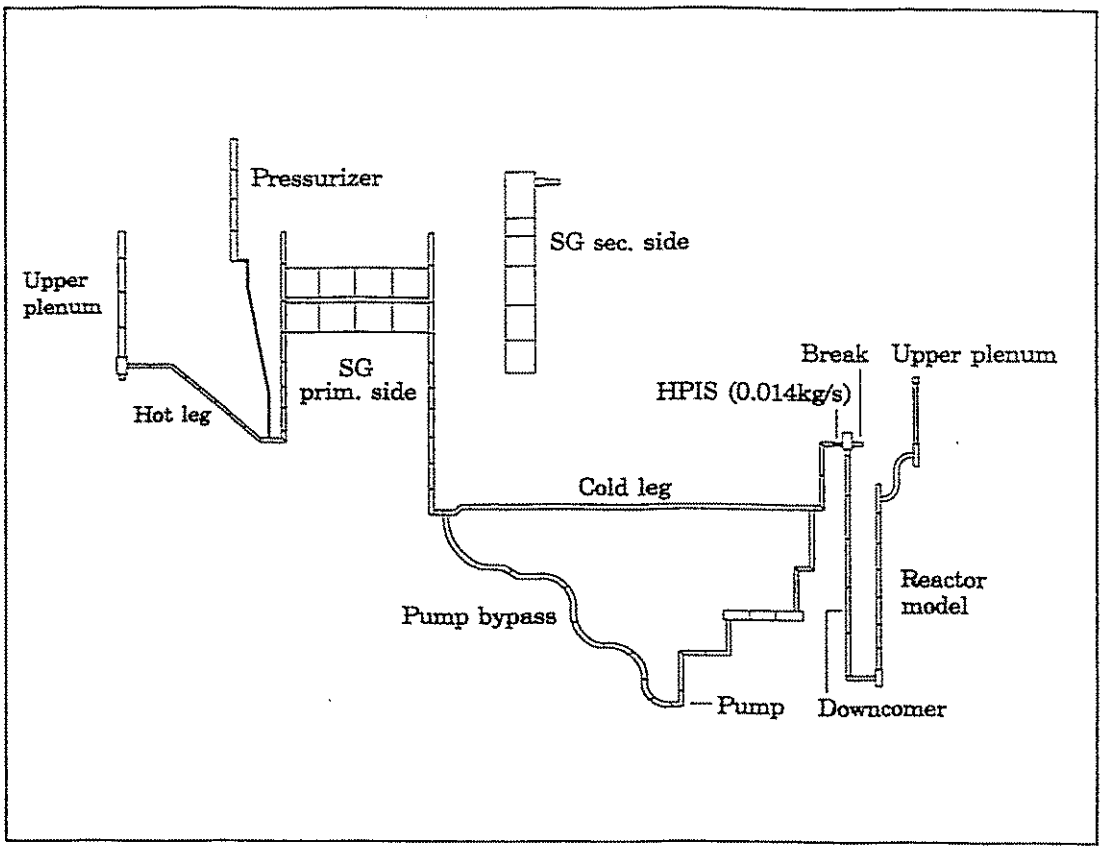

Fig. 5.1: Nodalization scheme of PMK-2 facility

5.2 Results

An overview about the experiment and the main events is given in chapter 3 and 4. In this chapter special features of the ATHLET calculation are discussed. The results of the calculation are given in Fig. 4.1 - 4.22. Additional for the ATHLET calculation in this chapter a comparison between the measured and calculated void fraction is given (Fig. 5.4-5.10). The locations of the void fraction sensors can be seen in Fig. 2.10. An overview about the measured and calculated main occurrences is presented in Table 5.1.

In Fig. 4.8 the primary pressure is shown to be depended on time. At beginning of the calculation the break valve opens and PV21, 22 closes (isolation of the steam generator secondary side). By opening the break valve a fast decrease of the system pressure is calculated. This pressure decrease is accelerated due to the start of SCRAM. Because of the continuous heat transfer from primary to secondary side in the first 90 s the secondary pressure (PR81, Fig.4.9) increases and the SG relief valve opens. After t=165s the SG relief valve is closed. By reducing heat transfer to secondary side the decrease of primary pressure is reduced (at appr. t=160s). After that the first of evaporation in the core leads to a slow increase of the primary pressure (t=550s). The pressure behaviour especially in the first 200s is influenced by modelling of the pump coast down.

At appr. t=500s the level in the inclined part of the hot leg (LE31, Fig.4.12) starts to drop. At t=750s level LE31 reaches the bottom of the loop seal and so steam is able to enter the SG hot collector. Caused by the loop seal clearing the primary pressure decreases after a local maximum (Fig.4.8).

	Experiment	Calculation
Break valve opens at	0.0s	0.0s
SCRAM initiated at	65s	57s
Pump coast down starts at	74s	80s
Start of HPIS at	65s	58s
SG relief valve opens at	41s	38s
SG relief valve closes at	150s	165s
Begin of dryout in the core at	1740s	1815s
End of dryout in the core at	1870s	1875s
End of experiment at	3998s	4000s

Tab. 5.1: Main occurrences and comparision with the experiment

After that both calculation and experiment show oscillations in the primary pressure, the levels (Fig.4.10, 4.12-4.14) and the flow rate (FL53, Fig.4.20) with approximately the same time period. The results of the calculation show that the reason for this kind of oscillations is the evaporation in the reactor model and the condensation of steam in the SG inlet.

As a consequence of condensation in the SG inlet the primary pressure decreases. The steam flow from the reactor to the SG leads to an increase of the mass flow (FL53) and also the reactor level (LE11) increases. The rise of the reactor level leads to a decrease of the void fraction in the reactor outlet and

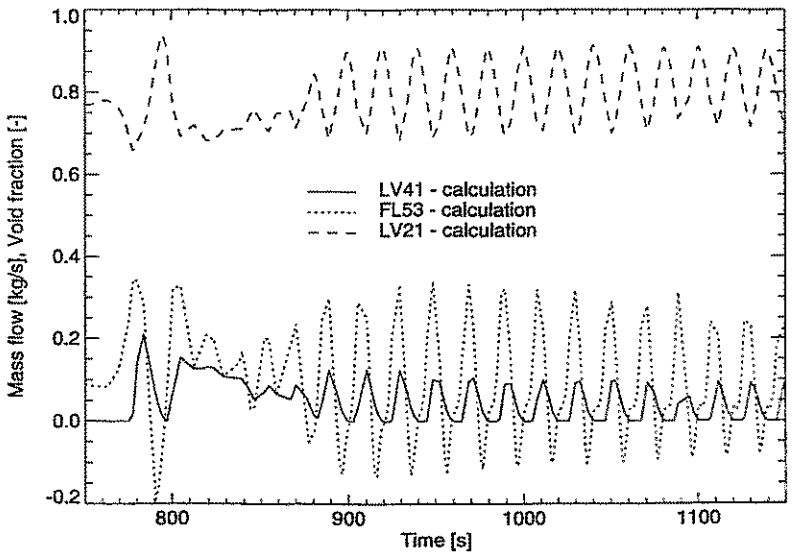

Fig. 5.2: Mass flow (FL53), void fraction at reactor outlet (LV21) and SG inlet (LV41)

as a result there is less condensation in the SG. As shown in Fig. 5.2 and 5.3 the primary pressure reaches a local minimum and for a short period the mass flow (FL53) is negative. The calculation shows there is a fluid mass flow directed from the SG inlet to the hot leg and so the hot leg loop seal is refilled. Once more the primary pressure increases and the described process is repeated periodically.

During the experiment an extended dry out period in the core takes place. This dry out phenomena connected with a high temperature excursion is also calculated by the ATHLET-code. Because of the decrease of the reactor level the cladding temperature (TE15, Fig.4.2) rises from 540K to appr. 610K (690K in the experiment). If the reactor level reaches it's minimum (LE11, Fig.4.10) the level in the cold leg reactor side starts to drop (LE52, Fig. 4.16). Already at t=1540s the level in the cold leg SG side (LE51, Fig. 4.15) starts to drop and reaches it's minimum at t=1850s. By the steam flow out of the SG, fluid from the cold leg flows directly to the core. The reactor level rises again and so the dry out period is limited. In the calculation the dry out period occures 75s later.

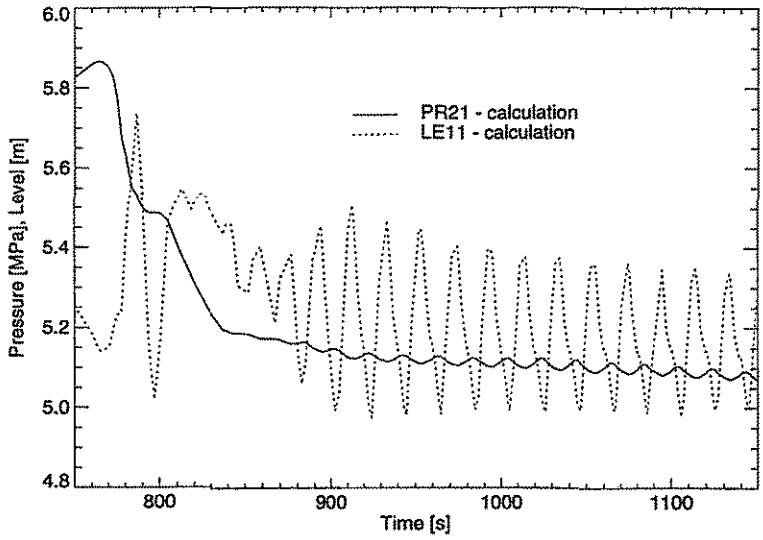

Fig. 5.3: Primary pressure (PR21) and reactor level (LE11)

When level LE51 reaches it's minimum the cold leg loop seal clearing takes place. Steam passes through the horizontal part of the cold leg and level LE52 decreases. After the cold leg loop seal clearing the break mass flow (FL01, Fig.4.21) is nearly equal to the mass flow from HPIS. Thereby to the end of the calculated transient the reactor level stagnates at approximately 2m.

The calculated results of the void fraction, presented in Fig. 5.4-5.10, show a qualitatively good agreement with the measurement data obtained from the needle shaped conductivity probes. Bearing in mind the fact that the measured values give an information about the local void fraction and the ATHLET code calculates a average void fraction for one node, deviations between measured and calculated values can be explained. The start of evaporation in the core at appr. t=200s can be seen in both calculation and experiment (Fig. 5.4, 5.5). At t=700s the mixture level reaches the position of LV34 in the inclined part of the hot leg (Fig. 5.6) and at appr. t=760s steam reaches the SG hot collector. The hot leg loop seal clearing can be observed in the results of LV41 (Fig. 5.7). Steam in the SG cold collector (LV42, Fig. 5.8) is not detected until t=1200s (1460s in the experiment). At t=1750-1850s the cold leg loop seal clearing takes place, as seen in the results of LV51 and LV52 (Fig. 5.9-5.10).

The given comparision between calculation and experiment shows, that all main occurences, e.g. the time behaviour of primary and secondary pressure, the hot and cold leg loop seal clearing, the dry out period in the core, are calculated very well by the ATHLET-code. Especially the correct calculation of oscillations concerning the hot leg loop seal clearing pleads for the applicability of the code ATHLET in order to calculate such kind of phenomena.

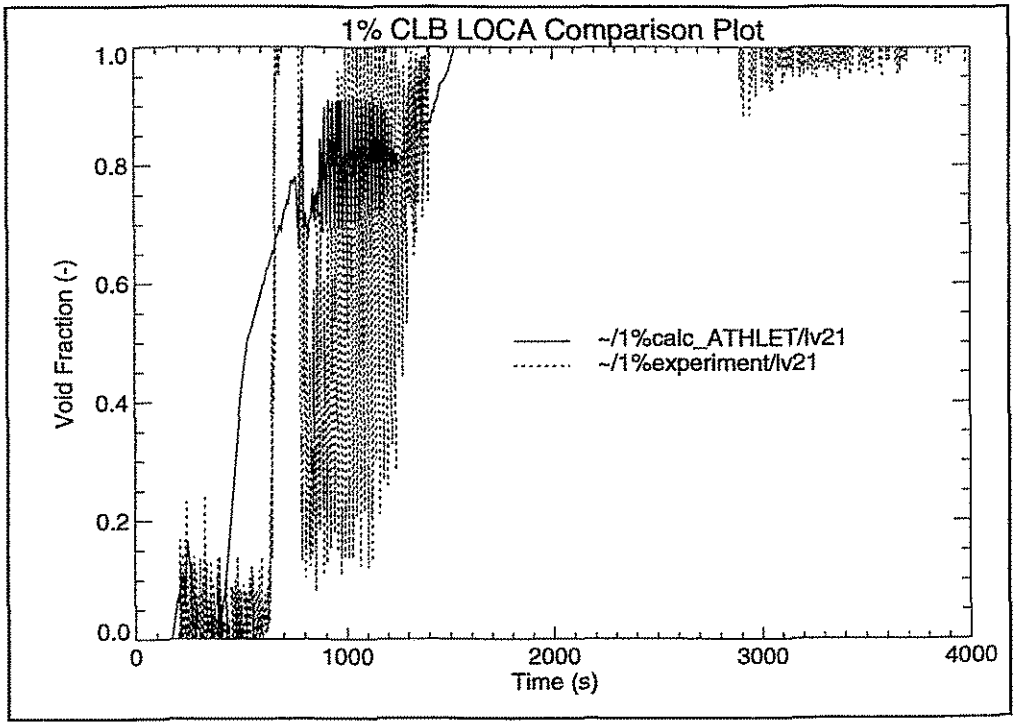

Fig 5.4: Void fraction in reactor outlet

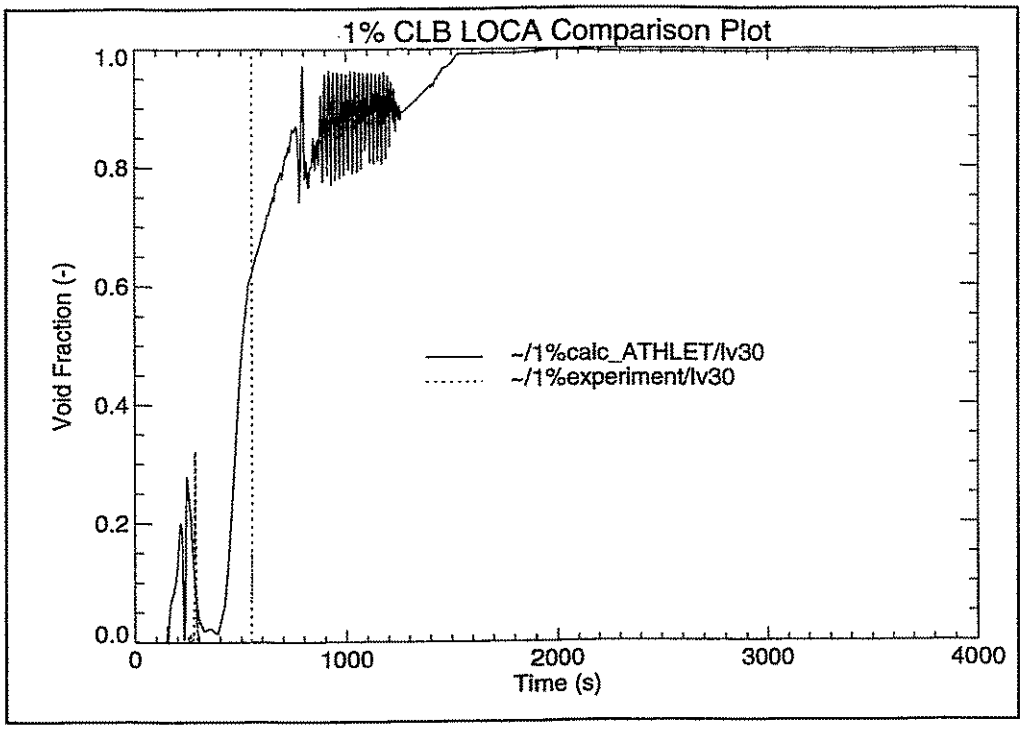

Fig 5.5: Void fraction in hot leg

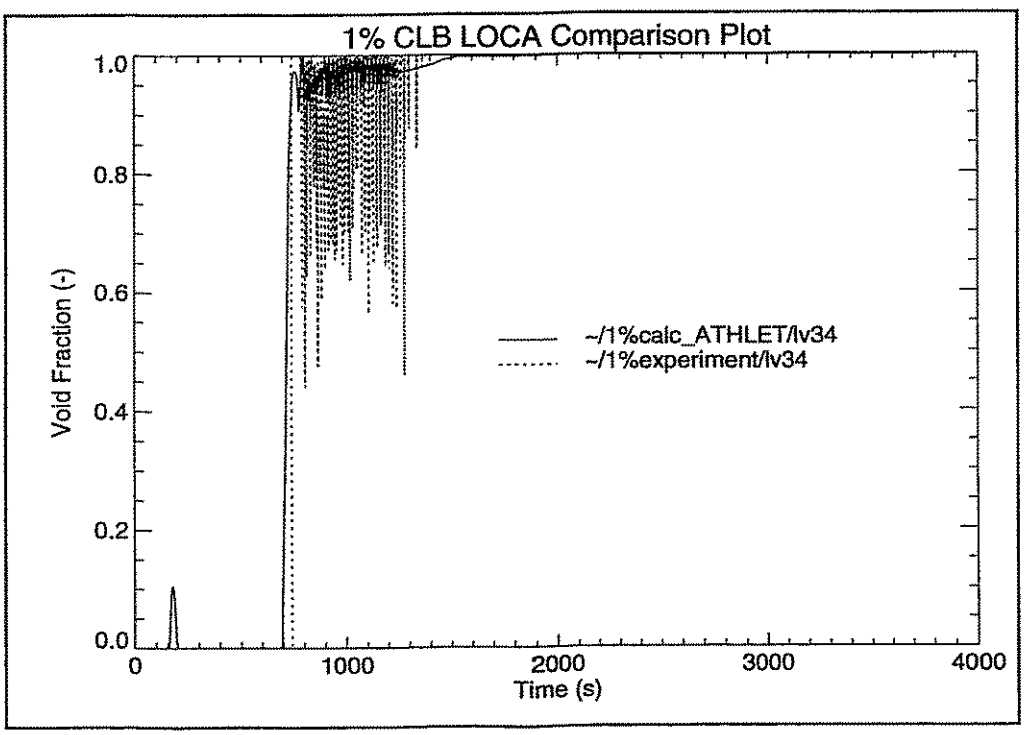

Fig. 5.6: Void fraction in hot leg inclined part

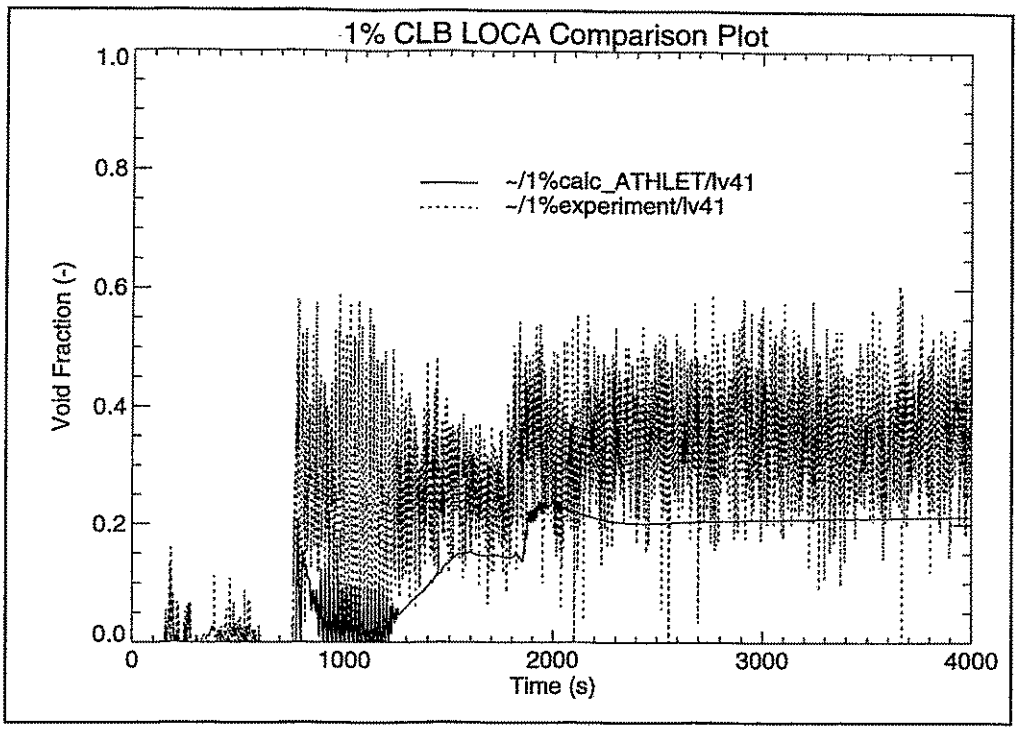

Fig. 5.7: Void fraction in SG inlet

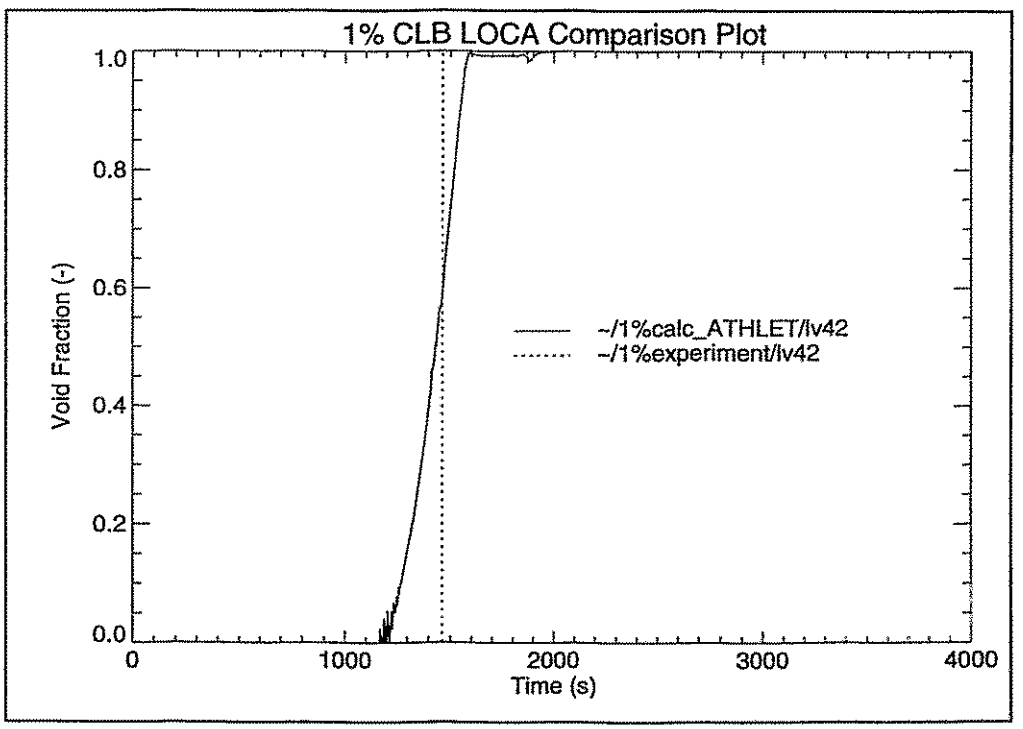

Fig. 5.8: Void fraction in SG outlet

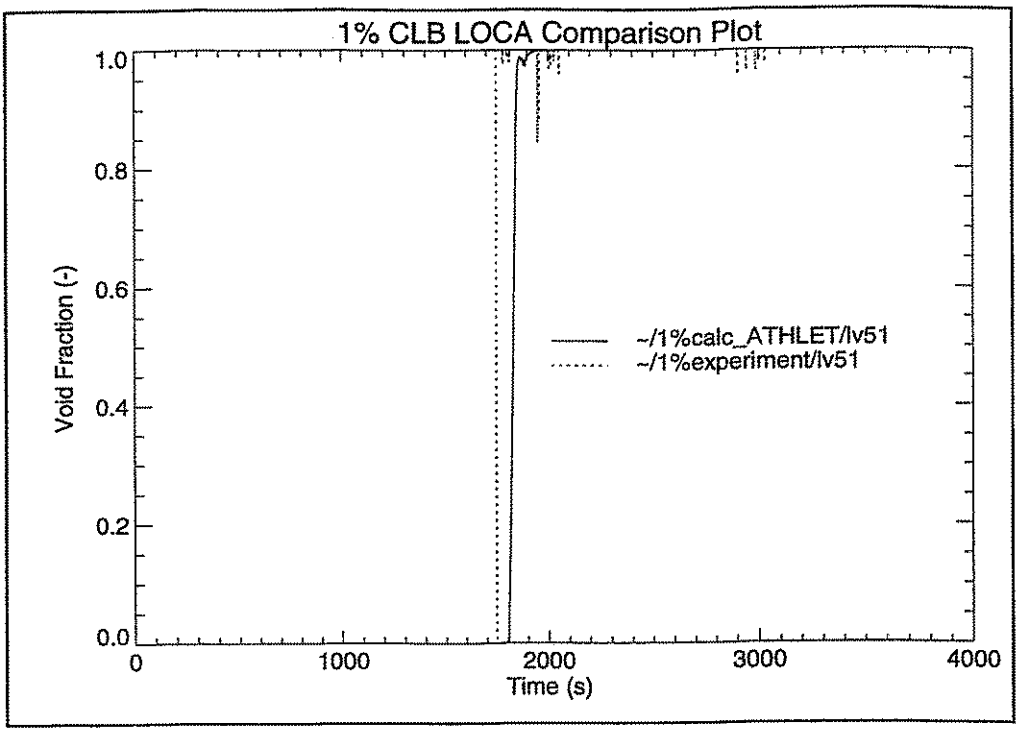

Fig 5.9: Void fraction in cold leg SG side

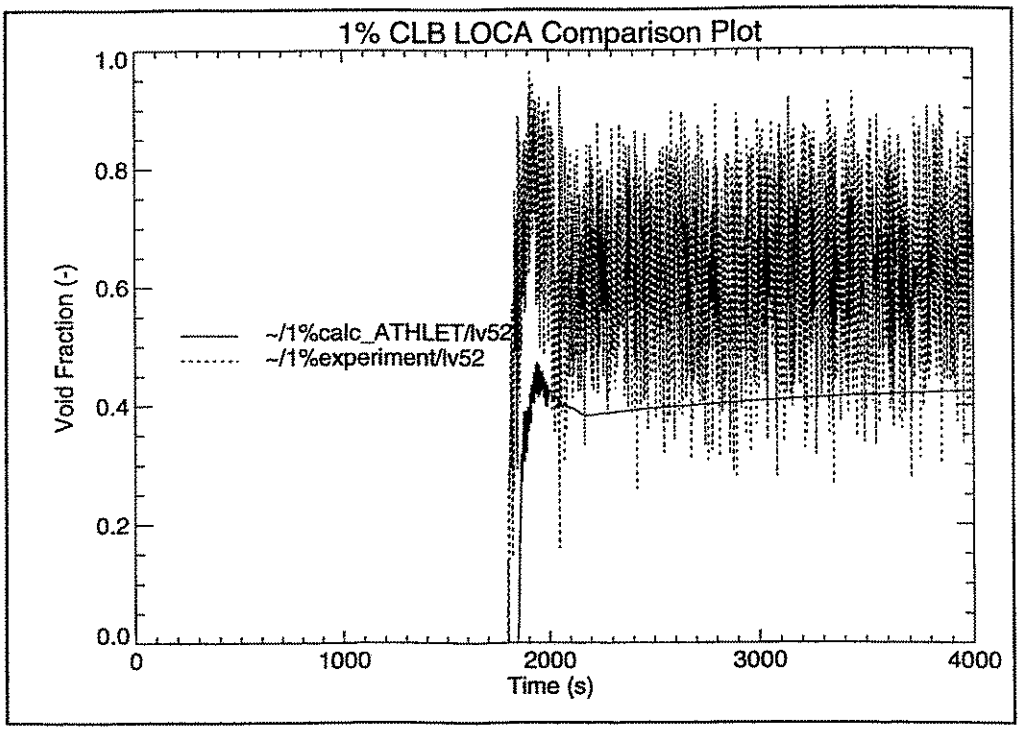

Fig. 5.10: Void fraction in cold leg reactor side

6. RELAP5 calculations

The post-test RELAP5 calculation have been performed by use of the code version RELAP5/MOD3.1 available in the framework of the international CAMP program of the US NRC and implemented at the KFKI Atomic Energy Research Institute on the IBM RISC-6000 type computer.

6.1 Modelling of the experiment

The nodalization of the PMK-2 facility used for the calculation is shown in Fig. 6.1. The nodalization scheme consists of 109 volumes including 12 time dependent volumes, 118 junctions including 5 time dependent junctions and 82 heat structures with 355 mesh points.

Table 6.1.

Group of components	Component numbers	Number of nodes
Hot leg	100-112	6
Primary side of steam generator	120-156	19
Cold leg from steam generator collector to pump simulator bypass	160-165	3
Pump coast down valve MV11	190	-
Pump isolation valve MV12	192	-
Pump simulator bypass tubes	166-174	6
Pump flow controller valve PV11	191	-
Cold leg from pump simulator to downcomer	175-183	6
Reactor vessel	200-250	24
Pressurizer, spray and surge line	400-430	8
HPIS system	620-621	1
LPIS system	622-625	2
SITs system	660-685	4
Feedwater simulation	580-582	2
Auxiliary feedwater	590-596	4
Secondary side of steam generator	500-550	12
Secondary steam line volumes	570-577	3
Secondary safety systems	599-615	3

Fig. 6.1 Nodalization scheme
for RELAP5/mod3.1

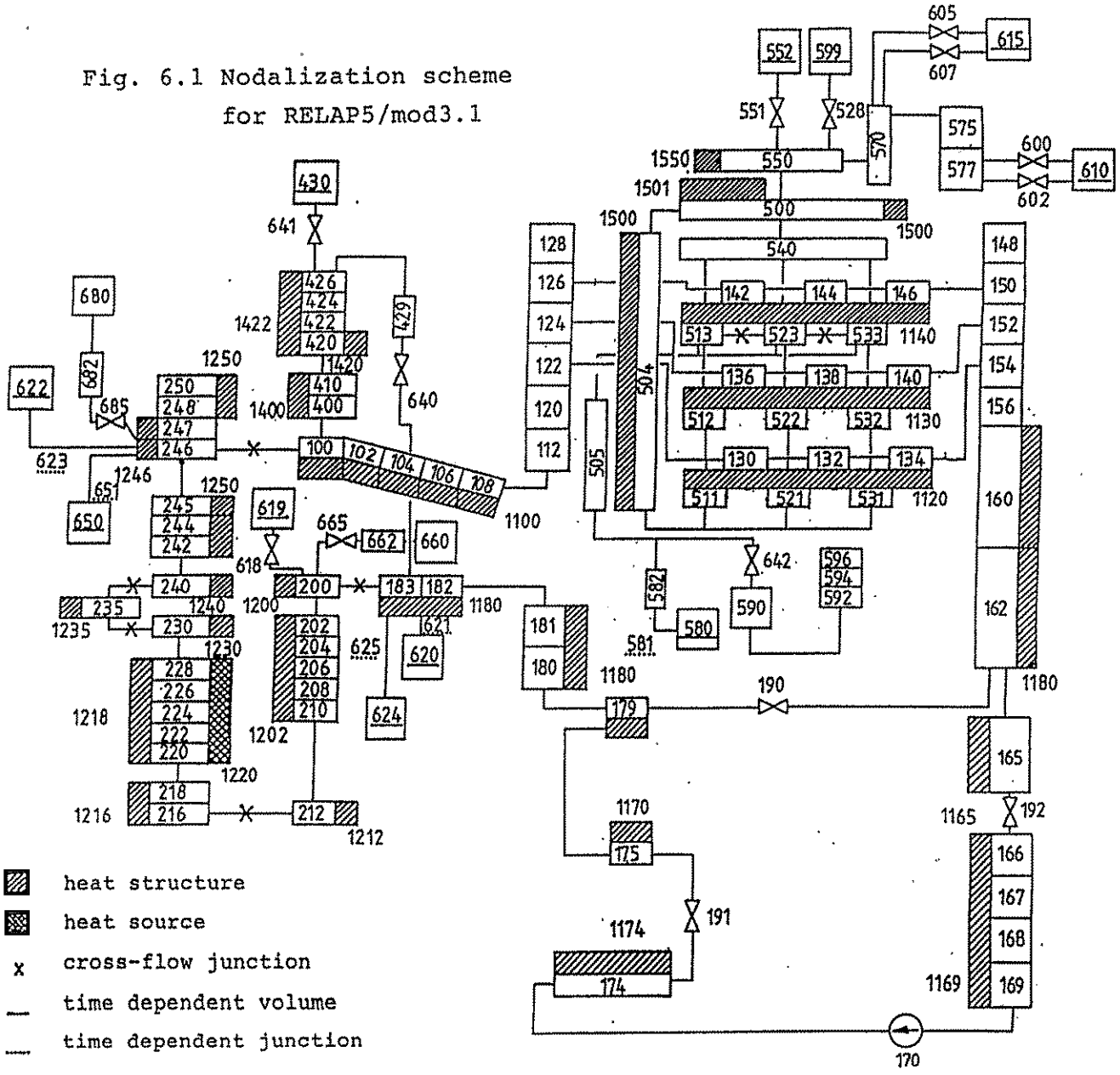

This nodalization scheme is derived from the scheme used for IAEA-SPE-4 [4] analyses (see Table 6.1). The modified scheme considers break as a BREAK VALVE (618). To model both the SG relief valve and the safety valve trip valves were used (600, 605).

Few cross flow junctions have been used to model the most critical connections of the facility:

- cold leg - downcomer head,
- downcomer - vessel,
- upper plenum 1 - upper plenum 2,
- upper plenum 2 - upper plenum 3,
- upper plenum 6 - hot leg,
- SG secondary - at feedwater injection level.

The steady state control system for pressurizer pressure was used to achieve the desired initial conditions for the transient calculation. The end of the steady-state calculations was at 100 s process time.

The main parameters at the end of the steady-state calculation are presented in Table 6.2.

Table 6.2.

Calculated and measured initial conditions

Parameter	Calculated	Measured
Pressure in upper plenum	12.46 MPa	12.43 MPa
Loop flow	5.10 kg/s	5.10 kg/s
Core inlet temperature	540.4 K	536.4 K
Core outlet temperature	565.2 K	565.0 K
Core power	658.1 kW	658.0 kW
Collapsed coolant level above bottom pressure tap of pressurizer	9.08 m	9.02 m
Primary coolant mass	139.6 kg	-
Secondary side pressure	4.50 MPa	4.51 MPa
Collapsed SG level above bottom pressure tap	8.06 m	7.83 m
Feedwater flow	0.350 kg/s	0.348 kg/s
Feedwater inlet temperature	496.2 K	496.2 K

Value used for both subcooled and two-phase discharge coefficients of break junction is 0.85. Loss coefficient in break junction is 5.0.

For the heat losses convective boundary condition was calculated in all wall heat structures with a heat transfer coefficient of 5 W/Km^2.

6.2 Results

The occurences outlined the accident process derived from the measurement and the calculation are summarized in Table 6.3.

The calculated results are presented in Figs. 4.1-4.12 in Chapter 4. The comparison of the calculated and measured quantities make easy the discussion of the computer modelling.

The calculated and measured values of the system pressures (PR21) are presented in Fig. 4.8. The prediction is qualitatively acceptable. The divergence is a consequence of the seconary pressure, which shows a much higher level in the calculation as in the experiment, as it can be seen in Fig. 4.9.

Table 6.3.

Occurences		Timing (s)	
		Measured	Calculated
0	Break valve opens	0	0
1	SG relief valve opens	41	24.8
2	Scram and HPIS flow initiated	65	63.6
3	Pump trip simulation initiated	74	75.3
4	SG relief valve closes	150	109.8
5	Pressurizer empty	180	145
6	Level in upper plenum drops to hot-leg elevation	640	504
7	Hot-leg loop seal cleared	750	762
8	Core uncovery begins	1737	-
9	Cold-leg loop seal cleared	1806	1765
10	Break flow two-phase	2110	1798
11	Test terminated at	3998	4000

The hot leg loop seal clearing in the calculation appears at 762 s (it is practically at same time, at 750 s in the experiment), when there is a local maximum on the pressure curve. This statement is evidenced by the hot leg loop seal reactor side level as shown in Fig. 4.12, by the coolant temperature in the upper plenum (Fig. 4.4) and by the coolant temperature at SG inlet (Fig. 4.5).

The cold leg loop seal clearing appears in the calculation at 1765 s (it is at 1806 s in the measurement). It can be seen in the cold leg loop seal level reactor side (Fig. 4.15) and cold leg loop seal level SG side (Fig. 4.14), while its effect can be find in the coolant temperature at the downcomer inlet (Fig. 4.3) and in the reactor model level (Fig. 4.10).

After the cold leg loop seal clearing the process can be qualified as a quasi-steady state process: practically there is no variation in the coolant levels.

As shown in Figs. 4.1 and 4.2, the extended dryout observed in the measurement cannot be predicted by the code. Looking at the details of the calculation it can be seen that there is no complete phase separation in the core region.

7. Comparison of the results

The results of the experiment and both calculations are described in chapters 4-6. In this chapter only the main events in the experiment and in the calculations are discussed. The main phenomena in the experiment are the hot leg loop seal clearing, the oscillations in flow rates and levels, the dryout period and finally the cold leg loop seal clearing.

After opening the break and the initiation of SCRAM a fast depressurization can be seen in the primary pressure behaviour (Fig. 4.8). In this time a fast increase on the secondary pressure (Fig. 4.9) can be observed, reaching the setpoint of the steam generator relief valve (PV23). The decrease of the primary pressure is reduced by a lower heat transfer to the secondary side, after closing the valve PV23. In the calculations there is a good agreement, qualitatively, in the primary pressure up to appr. t=200s. Deviations between the ATHLET calculation and the experiment are caused by the influence of modelling the pump coast down. Because of the higher heat transfer from the primary to the secondary side, in the RELAP5 calculation the steam generator relief valve (PV23) opens again for a short perid at t=261 s. Evaporation in the core leads to an increase in the primary pressure after appr. t=600 s and the hot leg loop seal level (LE31, Fig.4.12) begins to decrease. After reaches it's minimum, the hot leg loop seal clearing takes place.

Connected with the hot leg loop seal clearing, in the experiment and also in both calculations significant oscillations can be observed. An explanation of the oscillations is given in chapter 4 and related to the ATHLET calculation in chapter 5.2. During the oscillations the reactor level (LE11, Fig.4.10) stagnates at appr. 5.5m and level LE45 (Fig.4.13) decreases up to the end of oscillations. Than the break changes its suction direction, LE11 begins to decrease, while the LE45 remains constant. Because of the hot leg loop seal clearing, the primary pressure decreases after reaching a local maximum. This effect is calculated very well by the ATHLET and the RELAP5 codes.

The last significant event is the cold leg loop seal clearing. In the experiment at appr. t=1500s the cold leg level SG side (LE51, Fig.4.15) starts to decrease and drops to a absolute minimum. After reaching this minimum the cold leg loop seal clearing takes place. At the same time period the cold leg level reactor side decreases very fast. In both calculations a sharp pressure decrease can be observed, caused by condensation effects during a partly refilling of the core.

The ATHLET calculation in this part deviates from the experiment, therefore the reactor level (LE11) reaches a lower minimum. In this way the dryout period can be modelled by the ATHLET code. In the calculation the dry out occures at t=1815s instead of t=1740s in the experiment. Although level LE11 reaches a very low minimum, a dry out in the cladding temperatures is only calculated in the upper part of the core (TE15, Fig.4.2). The RELAP5 code calculates the correct levels, but the code is unable to predict the dryout period (Figs. 4.1, 4.2).

As seen in LE11 (Fig.4.10), DP11 (Fig.4.18) and LE52 (Fig.4.16), after the cold leg loop seal clearing a similar type of oscillations like after the hot leg loop seal clearing can be observed in the experiment and also in the ATHLET calculation. This oscillations are not calculated by the RELAP5 code.

Up to the end of the experiment there is practically a balance between the mass flow out of the break and the HPIS mass flow. The primary pressure decreases slowly and the reactor level (LE11) stagnates approximately at a constant value. In contrast to the experiment both codes calculate a significant increase of the level in the SG hot collector (LE45, Fig.4.13) after the cold leg loop seal clearing. The other coolant levels remain approximately constant. After the hot leg loop seal clearing the mass flow in the loop (FL53, Fig.4.20) is practically near by zero, except the time period of oscillations.

8. Conclusions

The 1% cold leg break experiment, described in this report, is one part of the co-operation between the Research Center Rossendorf, Germany (FZR) and the Atomic Energy Research Institute, Hungary (KFKI). The experiment, executed at the PMK-2 test facility in Budapest, is used for the verification of thermohydraulic computer codes. The post test calculations are performed by the ATHLET code on a Sun Workstation SPARC 10/40 (FZR) and by the RELAP5 code on a IBM RISC-6000 type computer (KFKI).

Generally both the ATHLET and RELAP code are able to calculate all main phenomena of the experiment, with exception of the dry-out-period in the core (RELAP5). The calculated results show a good agreement with the measured data. Especially effects, typical for VVER-440 reactors, are calculated very well.

For a better understanding of the experimental results the local void fraction sensors, developed by the FZR, are very usefull. The sensors provide more detailed information about evaporation, condensation and other two-phase flow phenomena.

Further experiments are intended to investigate the code capabilitys, i.e. a 1% cold leg break experiment with primary bleed and a 1% cold leg break experiment with hydroaccumulator injection.

9. References

[1] Simulation of a Loss of Coolant Accident. Results of a Standard Problem Exercise on the Simulation of a LOCA.
IAEA-TECDOC-425. Vienna, 1987

[2] Simulation of a Loss of Coolant Accident with Hydroaccumulator Injection. Results of the Second Standard Problem Exercise on the Simulation of a LOCA.
IAEA-TECDOC-477. Vienna, 1988

[3] Simulation of a Loss of Coolant Accident with a Leak on the Hot Collector of the Steam Generator. Results of the Third Standard Problem Exercise.
IAEA-TECDOC-586. Vienna, 1991

[4] Simulation of a Loss of Coolant Accident. Results of the Fourth IAEA Standard Problem Exercise.
IAEA-TECDOC. in preparation

[5] L. Perneczky, G. Ézsöl, L. Szabados: 1% Cold Leg SBLOCA Analysis on PMK-NVH Facility. Central Research Institute for Physics, Budapest, 1990

[6] Prasser, H.-M., Küppers, L., May, R.: Conductivity Probes for Two-Phase Flow Pattern Determination During Emergency Core Cooling (ECC) Injection Experiments at the COCO Facility (PHDR). Proceedings of the 1. OECD (NEA) CSNI - Specialist Meeting on Instrumentation to Manage Severe Accidents, Cologne, Germany, Juli 1992, NEA/CNSI/R(92)11, P. 273-289

[7] Prasser, H.-M., Zippe, W., Baldauf, D., Szabados, L., Ézsöl, Gy., Baranyai, G., Nagy, I.: Two-Phase Flow Behaviour during a Medium Size Cold Leg LOCA Test on PMK-II (SPE-4)
Jahrestagung Kerntechnik 1994, Stuttgart, Germany, Proceedings ISSN 0720-9207